Micro-Encapsulated Phase Change Materials: A Review of Encapsulation, Safety and Thermal Characteristics

Ahmed Hassan *, Mohammad Shakeel Laghari and Yasir Rashid

College of Engineering, United Arab Emirates University, Al-Ain P.O. Box 15551, UAE;
mslaghari@uaeu.ac.ae (M.S.L.); yasir.rashid@uaeu.ac.ae (Y.R.)
* Correspondence: ahmed.hassan@uaeu.ac.ae; Tel.: +971-56-8695917

Abstract: Phase change materials (PCMs) have been identified as potential candidates for building energy optimization by increasing the thermal mass of buildings. The increased thermal mass results in a drop in the cooling/heating loads, thus decreasing the energy demand in buildings. However, direct incorporation of PCMs into building elements undermines their structural performance, thereby posing a challenge for building integrity. In order to retain/improve building structural performance, as well as improving energy performance, micro-encapsulated PCMs are integrated into building materials. The integration of microencapsulation PCMs into building materials solves the PCM leakage problem and assures a good bond with building materials to achieve better structural performance. The aim of this article is to identify the optimum micro-encapsulation methods and materials for improving the energy, structural and safety performance of buildings. The article reviews the characteristics of micro-encapsulated PCMs relevant to building integration, focusing on safety rating, structural implications, and energy performance. The article uncovers the optimum combinations of the shell (encapsulant) and core (PCM) materials along with encapsulation methods by evaluating their merits and demerits.

Keywords: microencapsulation; thermal energy storage; phase change materials; thermally activated building systems

1. Introduction

Phase change materials (PCMs) are considered to be potential energy saving materials since, due to latent heat absorption, they can substantially increase the thermal mass of buildings compared to conventional building materials presented in Figure 1 [1].
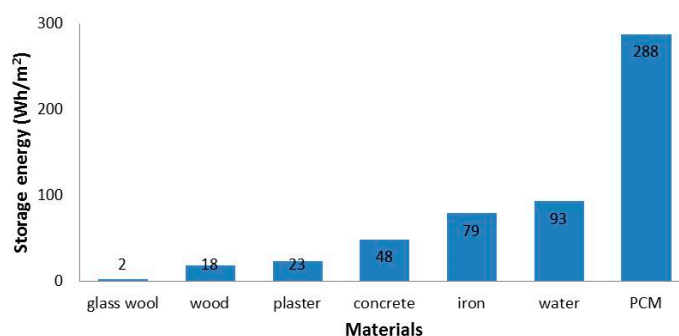

Figure 1. Comparison of the maximum energy storage capacity of 10 mm thickness of different building materials operating between 18 °C and 26 °C for 24 h [1].

Phase change materials have been extensively reviewed in terms of their classifications, thermo-physical properties, applications and impact on the energy performance of buildings [2–6]. The previous reviews have mainly identified three types of PCMs for incorporation into buildings to reduce their energy consumption, namely paraffin waxes, salt hydrates and fatty acids, summarized in Figure 2.
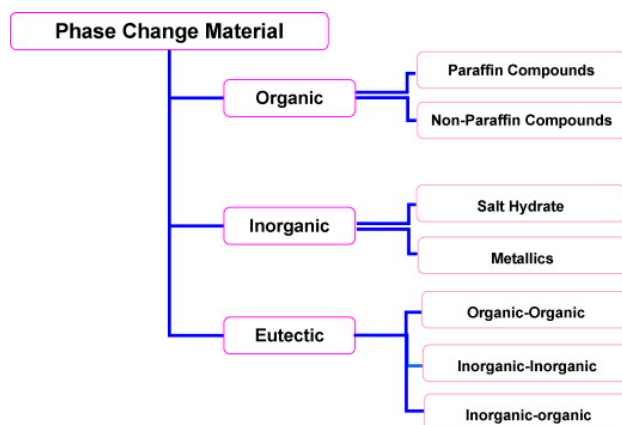

Figure 2. Classification of phase change materials (PCMs) conventionally applied for latent heat storage in buildings [3].

As the concept has developed, the more recent reviews have focused on the improvement in PCM properties, different ways of integration into buildings and PCM behaviors in a built environment. Liu et al. reviewed the thermal conductivity enhancement to increase the charging/discharging rate of the PCM used in building application to increase energy efficiency and achieve better indoor thermal comfort. This review summarized the carbon based and metal based conductivity enhancers. Carbon based additives include carbon fibers, Nano-tubes, carbon foam, graphite, graphite powder, graphene. Metal based additives include particles and or containers of aluminum, copper, nickel and gold particles and metal salts. This review also compiled the models to calculate thermal conductivity [7]. J. Pereira da Cunha and P.C. Eames reviewed microencapsulated PCMs with a melting point range of 0 °C to 250 °C including organic PCMs, salt hydrates and eutectics as heat transfer fluids in heat exchangers. This review summarized the applications of encapsulated PCMs in active heating/cooling systems as a means to increase heat transfer rates [8]. M. Jurkowska and I. Szczygieł reviewed PCMs as heat transfer enhancers prepared as slurries and suspensions. They particularly focused on the stability, durability and hydrodynamic properties of such PCMs [9]. Akeiber et al. summarized different types of phase change materials for building applications with the melting points within the thermal comfort zone. They reviewed thoroughly the integration of PCMs into the building components i.e., walls, roofs, windows and floors [10]. A. Kylili and P.A. Fokaides reviewed life cycle assessment of PCMs for building integration. Their work includes sustainability and environmental impact of these materials as compared to the conventional buildings [11]. Zhang et al. reviewed PCMs for thermal energy storage and thermal management applications mainly focusing on modeling of the effective thermal conductivities and methodologies to enhance heat transfer rates [12]. Silva et al. reviewed the application of PCMs in the windows and glazing of the buildings as an approach for building integration [13]. The previous reviews do not identify a suitable microencapsulation process for a particular PCM type, the effect of PCM toxicities on the built environment and the limitations of the PCM applicability into buildings considering the structural component. Conclusively, a comprehensive review is desired to identify the optimal microencapsulation process for a particular PCM. For example, a metallic shell would be less suited to encapsulate salt hydrates due to salt's affinity to corrode metals. On the contrary, a polymeric shell material is better suited for salt hydrates. On the other hand, the paraffin waxes, being non-corrosive, can be encapsulated equally in the metallic

and polymeric shell. There is also a lack of safety related issues of the PCMs (such as toxicity), as an important design parameter when it comes to PCM integration into buildings, as dwellings would be exposed to PCMs over a longer period of time and must be assured not to contract toxic elements during material preparation, construction and post-construction occupancy.

This current review is on the relevant and relatively less explored issues related to safety via toxicity, chemical interaction related properties (such as corrosion), suitability of the particular microencapsulation process for the specific PCMs and their structural and thermal performances. The review would evaluate PCMs' integration into buildings from a scientist's, designer's, construction manager's and policy maker's point of view, in view of their pre and post integration implication on buildings. The PCMs are critically reviewed for their suitability in building integration starting from PCM properties. A comprehensive description and detailed comparison of the encapsulation processes that would eventually affect their building integration in terms of structural performance of buildings is provided. The review links suitable types of shell material and encapsulation processes for certain core materials. The performance of PCMs, specific to PCM types integrated into building components, is summarized.

For predominantly hotter climates, PCMs can be selected with the melting point below the upper range of comfort zone so that it can melt during daytime and absorb excess thermal energy to restrict indoor temperature close to comfort. Similarly, in predominantly colder climates, the PCM melting point should be above the lower limit of the comfort zone to store and supply heat for space heating near comfort [14]. In the case of improper selection of a PCM melting point, with regard to the ambient temperature at nighttime, PCMs may not regenerate to solid, and absorb heat during the next day, thereby undermining their effectiveness [15,16].

Initially, PCMs were integrated into buildings by impregnation [17–19], immersion [20] or direct incorporation [21] of PCM into the porous aggregate of the concrete mix. The PCMs filled in porous aggregate can enhance concrete density and heat storage capacity resulting in enhanced thermal inertia [19]. However, all these methods suffered through leakage of PCM with the passage of time [22]. The leaked PCM would react with the building material leading to corrosion, along with affecting strength, thereby reducing building life [23]. An approach to solve the aforementioned issue is to contain PCMs in a suitable shell material leading to the development of microencapsulated PCMs [24].

Encapsulation is a technique to cage the required material inside another shell material to achieve desired characteristics of preservation, time-dependent release of material, delivery of the substance to the specific target, reduction of reactions to the environment, prevention of corrosion, the stability of function and to facilitate the use of toxic materials [25,26]. The caging shell covers and protects the core material from the external environment to facilitate the desired application. Microencapsulation technology is applied in major fields such as medicine, food preservation, thermal energy storage, cosmetics, textile, and defense [27–31]. To benefit from this technique, technology was further improved to encapsulate such materials that are small in diameter, in the range of micrometers, thereby called microencapsulation [32]. The characteristics desired or achieved through microencapsulation for building applications are summarized in Table 1. In the sections below, the characteristics of each class of core materials (PCMs) are discussed with suitable shell materials depending on different applications.

Table 1. Desirable characteristics for microencapsulation, shell material, and PCMs.

Microencapsulation	Shell Material (Encapsulant)	PCM
Increased heat transfer efficiency	Flexible, thermally stable, and resistant to corrosion	Stability over several thermal cycles comparable to building life
Increase heat transfer area	Protection of the PCM from direct exposure to outside environment	Corrosion resistant with shell material

Table 1. *Cont.*

Microencapsulation	Shell Material (Encapsulant)	PCM
Eliminate reaction of core material with outside environment	Conductive for active energy storage and insulating for incorporation into building components	Conductive for active thermal energy storage systems and insulating for incorporation into building components
Accommodate volume changes during phase transition	Good bonding with both the PCM and the construction material	Phase transition temperature close to comfort zone
Easy handling	Non-toxic	No sub-cooling
Fine distribution	Low cost	No incongruent melting
[33–35]	Fire resistant	Non-toxic
	Nonhazardous [24]	Low cost
		Fire resistant
		Nonhazardous
		Reversibility of phase transition
		Re-usable [36–38]

2. Optimum Core (PCM) and Shell (Encapsulant) Materials

The choice of a core material (PCM) depends on the application, with the heat of fusion, density, thermal conductivity, heat capacity, toxicity, corrosion and fire resistance being potentially important. Since different PCMs exhibit different toxicological and interaction properties, it is extremely important to evaluate such properties in order to identify suitable shell materials (encapsulant). The Sections 2.1–2.4 briefly review the PCM properties which impact on the choice of optimal encapsulant material. Section 2.5 reviews commercially available PCMs and their encapsulant materials.

2.1. Paraffin Waxes

Paraffin waxes are by-products of petroleum and are abundantly available at quite a low cost of $4/kg [39]. Paraffin waxes have favorable characteristics for thermal energy storage applications such as higher latent heat of fusion, up to 259 kJ/kg [40], a lower thermal conductivity of 0.2–0.4 W/m·K and reasonable solid density of 0.93 kg/L [41,42]. Paraffin exhibits no super-cooling, no incongruent melting and has the ability to self-nucleate [43] which improves their solidification behavior. Superior solidification properties make them the favorable candidate for building applications where complete solidification at nighttime, through efficient heat removal, guarantees maximum heat absorption on the proceeding day [44]. Paraffin remains structurally stable without derating their thermal energy storage capacity over several thousand cycles [45]. Paraffins are available in a wide range of the melting points, from −5 °C to 76 °C [3], which renders them suitable for a variety of applications related to the passive and active cooling of buildings [46].

Paraffins have been proved effective in heat storage in traditional building skin, resulting in a decrease in space cooling load in warmer climates and heating load in colder climates [47]. Advanced building skins composed of building integrated photovoltaic (BIPV) systems have also employed paraffin to control PV temperature and reduce heat gain in buildings [48]. The thermal energy stored in paraffin behind the PV can be utilized in various temperature ranges by an appropriate selection of a paraffin melting point [49,50].

Lower thermal conductivities of paraffin compared to conventional building materials such as concrete (1.8 W/m·K), ordinary clay bricks (1.4 W/m·K) and mortar (1.73 W/m·K) [42] imparts insulating effect on buildings when integrated into building materials [51]. The insulating effect further increases when the low conductivity core (paraffin) is encapsulated in an even lower conductivity shell, such as polymers (poly methyl methacrylate) with thermal conductivity 0.17 W/m·K to

0.25 W/m·K [42]. However, in colder climates, a higher thermal conductivity shell or core materials (paraffin with Nano-graphite—NG) are desired. The addition of 10% NG by weight is reported to increase the thermal conductivity of paraffin from 0.2 to 0.94 W/m·K [52]. The enhanced thermal conductivity increases the transmission of stored heat in PCMs to indoors at nighttime, thereby reducing space heating demand [53]. Paraffins show better contact to the surface of containment, showing a lower subtended angle with the surface, resulting in better heat transfer to/from the shell material [54].

The superscripts H, is hazardous in a particular form of transport, while NH is non-hazardous in any form of transport [55]. The downside of paraffin is the itching with polymers if exposed to air at elevated temperatures for prolonged durations [43]. Additionally, paraffins exhibit a lower flash point in the range of 108 °C to 170 °C [56] which makes their use in building vulnerable to fire. Therefore, a fire resistant shell material is crucially important to enable them to withstand the fire [57].

In recent developments, paraffins are encapsulated in newer shell materials such as (i) polystyrene [29], calcium carbonate [58] and urea formaldehyde [59]; (ii) in composites such as silicon dioxide/polystyrene—organic/inorganic hybrid [60] and polymethyl methacrylate/silicon nitride—organic/inorganic hybrid [61]. Paraffins are blended with different PCMs such as ester [62], carbon Nano-fibers and carbon Nano-tubes [63], physicochemical stabilizers [64], polymer shell combined with aluminum honeycomb [65], cement mortar [66] and melamine and epoxy resin [67] to attain suitable thermal and structural properties. Table 2 summarizes research-based paraffin PCMs with their thermo-physical properties and encapsulation methods.

Table 2. Thermo-physical properties of research-based paraffin and paraffin composites with shell materials and encapsulation methods.

Reported Material	Core Material	Shell Material	Heat of Fusion (KJ/kg)	Melting Point (°C)	Encapsulation Method
PS/(C24–C18) [29]	*N*-tetracosane [NH], *N*-octadecane [H] eutectic mixture	Polystyrene	72–156	25	Emulsion polymerization method
NG/paraffin PCM [52]	Paraffin [NH]	Nano-graphite	182–209	27–28	Dispersion method
N-octadecane PCM with CaCO$_3$ shell [58]	*N*-octadecane [H]	Calcium carbonate	47–84	23–29	Self-assembly method
Paraffin capsules [59]	Paraffin [NH]	Urea-formaldehyde	204–102	50–52	In-situ encapsulation
MePCM [60]	1-dodecanol [H]	PS/sio$_2$ organic–inorganic hybrids	92–115	24	Surfactant-free pickering emulsion polymerization
Silicon nitride [61]	*N*-octadecane [H]	Polymethyl methacrylate + Silicon nitride	121–122	27	Suspension-like polymerization method
Cellulose—PCM blends [62]	*N*-octadecane [H] + ester	NA	120	25–29	NA
Composite PCMs [63]	Paraffin [NH] and soy wax [NH]	Carbon Nano-fiber, Carbon Nano-tubes	NA	52–54	Mixing and melting techniques
Paraffin/EG composite [68]	Paraffin [NH]	Expandable graphite powder	NA	58–60	High-pressure compression
Paraffin-based Nano-composite PCMs [69]	Paraffin [NH]	S-MWCNTs L-MWCNTs CNFs GNPs	175–205	59	Melt-mixing scheme

Reported Material	Core Material	Shell Material	Heat of Fusion (KJ/kg)	Melting Point (°C)	Encapsulation Method
Binary composites for PCM [70]	Octadecane [H] paraffin [NH]	HDPE LDPE LLDPE	293–241	20–28	Blending
Silica encapsulation of N-octadecane [71]	N-octadecane [H]	Silica	125–123	NA	Sol–gel process
N-octadecane microcapsules [72]	N-octadecane [H]	Sodium silicate	22–71	23–27	Sol–gel process

Note: [NH] means: non-hazardous; [H] means: hazardous; NA means: information not available [55].

2.2. Organic Non-Paraffins (Fatty Acids)

Non-paraffin organic PCMs also have characteristics favorable for building applications including higher heat of fusion, up to 259 kJ/kg [3]; availability in a wide range of melting points, from 7.8 °C to 127.2 °C [3]; lower thermal conductivity, from 0.14 to 0.17 W/m·K [5]; and no super-cooling. In addition, they show solid–solid phase transition as which makes them unique compared to paraffin. The fatty acids and their appropriate encapsulation materials are summarized in Table 3.

Table 3. Thermo-physical properties of organics fatty acids mixtures with suitable shell materials and encapsulation method.

Reported Material	Core Material	Shell Material	Heat of Fusion (KJ/kg)	Phase Transition Point (°C)	Encapsulation Method
Natural coco fatty acid mixture [73]	coco fatty acid mixture	gum Arabic, gelatin powder, melamine, formaldehyde, urea, β-naphthol	NA	22–24	coacervation technique
Polynary fatty acid eutectic mixture [74]	Stearic acid Palmitic acid Myristic acid Lauric acid	Epoxy resin	152–169	27–28	Vacuum impregnation
Eutectics based on fatty acids [75]	Capric acid with other eutectics	Not encapsulated	100–160	20–30	Mixing process
Shape-stabilized PCMs [76]	Stearic acid	Titanium dioxide	48	54	Mixing process
Microencapsulated SA [77]	Stearic acid	Silicon dioxide	162–171	53–54	Sol–gel method
Caprylic acid with different wall materials [78]	Caprylic acid	Urea-formaldehyde resin Melamine-formaldehyde resin Urea + melamine-formaldehyde resin	94–106	15–17	Coacervation method
Solid–solid phase transition [79]	Pentaerythritol Pentaglycerine Cross-linked polyethene Neopentylglycol	Not encapsulated	323 16 192 130	188 81 140 43	NA

In addition to corrosion, some fatty acids are toxic or release toxic fumes at elevated temperatures [80], therefore, cannot be directly incorporated into the buildings without encapsulation [81] as listed in Table 4 [82].

Some PCMs show phase transitions beyond human comfort so they cannot be integrated into building materials. Instead, such PCMs can be included in the building skin via an active system such as solar collector, concentrator photovoltaic and high-temperature heat exchanger to deliver building energy demand [83].

Table 4. Corrosion effects observed with metals by metallographic examination after 910 thermal cycles.

Metals	Stearic Acid	Palmitic Acid	Myristic Acid	Lauric Acid
Steel C$_{20}$ [82]	Resistant	Slightly corroded	Slightly corroded	Resistant
Cu [82]	Slightly corroded	Slightly corroded	Slightly corroded	Slightly corroded

Table 5 highlights that fatty acids are toxic, however, they are still being used in micro-encapsulations without regard to their toxicity. Since most of the building codes may prohibit the use of such toxic materials, it is crucially important to be aware of their environmental and code compliance requirements before investigating their use in buildings.

Table 5. Toxicological level and rating of fatty acids.

Compound Name	Level of Toxicity	Institution Defining Toxicity
Phenol [80]	Highly toxic	Acute rating from U.S. EPA product label
Camphenilone [80]	Acute toxic	Acute rating from U.S. EPA product label
Benzamide [80]	Highly toxic fumes on heating	Acute rating from U.S. EPA product label
Formic acid [84]	Acute toxic	PAN pesticide database
Methyl palmitate [84]	Acute toxic	PAN pesticide database
Acetic acid [84]	Acute toxic	PAN pesticide database
Capric acid [84]	Acute toxic	PAN pesticide database
D-Lactic acid [85]	Slightly toxic	Medical hospital
Caprylone [86]	Varying level of toxicity	Journal paper
Oxalate [87]	Toxic	Examiner of alternative medicine
Cyanamide [88]	Toxic	Product description
Hypophosphoric acid [89]	Acute toxic	Chemical manufacturer—product description

2.3. Salt Hydrates

Salt hydrates have desirable characteristics of a higher density of 1640 kg/m^3 [90]; negligible (less than 1%) volume changes during phase change [91,92]; cheaper availability with an average cost of \$0.13–0.20/kg for calcium chloride [93,94]; higher heat of fusion of up to 296 kJ/kg [95]; higher thermal conductivity of 0.6 W/m·K [96]; and favorable transition temperatures in the range of 25 °C–34 °C [97]. The salt hydrates are abundantly available [98] in large quantities as by-products of industrial processes [95,99] and as waste co-products in many chemical processes including the production of soda ash [100].

The main problems with salt hydrates are their lower thermal stability [101,102], chemical instability [95], corrosion to metals [102,103], incongruent melting [101] and sub-cooling below the solidification temperature [103]. The incongruence can be solved by mechanical stirring [104], using excess water to prevent forming a supersaturated solution from melted crystals [105] and modification of their chemical composition [106,107]. Mechanical stability can be improved by PCM encapsulation to reduce separation [108]. Sub-cooling can be suppressed by the addition of thickening agents [109] and a nucleating agent such as borax [110]. However, high-density borax may settle down when added into PCM which may require further investigation to solve this problem [111,112]. Thermo-physical properties of salt hydrates with different shell materials investigated in literature are summarized in Table 6.

Table 6. Thermo-physical properties of salt hydrates with a suitable shell material and encapsulation method.

PCM	Core Material	Shell Material	Heat of Fusion (KJ/kg)	Melting Point (°C)	Encapsulation Method
PCM thermal shield [113]	Hydrated salt	Aluminum foil	150	31	NA
Heterogeneous composite PCMs [114]	^{H} LiNO$_3$, ^{NH} KCl LiNO$_3$, ^{H} NaNO$_3$ LiNO$_3$, ^{NH} NaCl	Expanded graphite	158–112 190–185 232–206	168–140 197–184 228–213	Solution impregnation method

Table 6. *Cont.*

PCM	Core Material	Shell Material	Heat of Fusion (KJ/kg)	Melting Point (°C)	Encapsulation Method
Microencapsulation of a hydrated salt [115]	[H] Disodium hydrogen phosphate heptahydrate	Poly methyl methacrylate	150	51	Suspension copolymerization-solvent volatile method
Manganese nitrate hexahydrate [116]	[H] $Mn(NO_3)_2 \cdot 6H_2O$	NA	126–148	25	NA
Lithium metaborate octahydrate [116]	[H] $LiBO_2 \cdot 8H_2O$	NA	289	26	NA
Calcium chloride hexahydrate [116]	[H] $CaCl_2 \cdot 6H_2O$	NA	170–192	29–30	NA
Calcium chloride dodecahydrate [116]	[H] $CaCl_2 \cdot 12H_2O$	NA	174	30	NA
Lithium nitrate trihydrate [116]	[H] $LiNO_3 \cdot 3H_2O$	NA	179–296	30	NA
Sodium sulphate decahydrate [116]	[NH] $Na_2SO_4 \cdot 10H_2O$	NA	251–254	32	NA
Sodium carbonate decahydrate [116]	[H] $Na_2CO_3 \cdot 10H_2O$	NA	267	32	NA
Iron potassium alum [116]	[NA] $KFe(SO_4)_2 \cdot 12H_2O$	NA	173	33	NA
Calcium bromide hexahydrate [116]	[H] $CaBr_2 \cdot 6H_2O$	NA	115–138	34	NA
Lithium bromide dihydrate [116]	[H] $LiBr \cdot 2H_2O$	NA	124	34	NA

Note: [NH] means: non-hazardous; [H] means: hazardous; NA means: information not available [55].

2.4. Low Melting Point Metals and Alloys

Low melting point metals and alloys (liquid at temperatures near comfort zone) are being used as PCMs with favorable characteristics such as a higher thermal conductivity of 29.4 W/m·K, a higher density of 5907 kg/m^3, higher thermal cycling stability for millions of cycles and a moderate heat storage capacity of up to 80 kJ/kg [36]. Heat storage capacity per volume of these materials is much higher as compared to the heat storage capacity per mass because of their huge density as compared to conventional PCMs [117]. These PCMs are currently studied for the cooling of electronic equipment [118,119], high power LEDs [120], heat exchangers [120] and for exergy from low-grade heat energy to produce electricity [121,122]. Thermo-physical properties of phase change metals and alloys are presented in Table 7.

Table 7. Thermo-physical properties of low melting point metals.

Classification	Core Material	Heat of Fusion (kJ/kg)	Melting Point (°C)
Low melting point liquid metal [36,123] Metal eutectics [117]	Cesium	16	29
	Gallium	80	30
	Rubidium	26	39
	Eutectics of Bi-Pb-Cd-Sn-In	25–100	30–125

2.5. Commercial PCMs

Table 8 contains commercial PCMs targeted for building applications with the melting point within thermal comfort. For most of these materials, shell or coating is not revealed by the manufacturers. The available characteristics are provided to help select a specific material for the certain application.

The overall merits and demerits of different types of PCMs are summarized in Table 9.

Table 8. Thermo-physical properties of commercially available micro-encapsulated PCMs.

Company Name	Product Name	Core Material	Shell Material	Encapsulation Method	Heat of Fusion (kJ/kg)	Melting Point (°C)
BASF—Micronal® PCM [124]	DS 5000–DS 5040	Wax mixture	Polymethylmethacrylate	Spray drying	37–110	21–26
Rubitherm GmbH [125]	RT 18–RT 35	Organic PCM	Polymer	Na	125–220	18–35
	SP 21–SP 31	Inorganic PCM	Polymer	Na	130–190	21–33
Microtek Laboratories, Inc. [126]	MPCM (18D–37D)	Paraffin	Polymer	Hybrid system	168–195	18–37
savEnrg™ Phase Change Material [127]	PCM-HS (22P–29P)	Mixture of salt hydrates	Na	Na	185–190	22–30
	PCM-OM37P	Bio-based organic			218	37
Phase Change Products Pty Ltd. [128]	PC (25–29)	Hydrated calcium and magnesium chlorides	Na	Na	150–188	25–29
PCM Energy P. Ltd. [129]	Latest™ (18T–29T)	Inorganic Salt	Na	Na	175	18–29
	Latest™ (32S–36S)				200–230	32–36
Phase Change Material Products Limited [130]	X 25, X 30	Solid–Solid	Na	Na	105–110	25–30
	A 22–A 36	Organic			130–226	22–36
	S 21–S 34	Salt Hydrates			115–200	22–34
Climator Sweden AB [131]	ClimSel™ C (21–28)	Hydrated sodium sulphate	Na	Na	134–170	21–31
Salca BV [132]	Thermusol HD (26–60)	Salt hydrate	Na	Na	145–150	26–60
Entropy Solutions, LLC. [133]	PureTemp (20–37)	Bio-based material	Na	Na	171–227	20–38

Table 9. Merits and demerits of different PCMs.

	Paraffins	Organic PCMs Fatty Acids	Salt Hydrates	Low Melting Point Metals
Advantages	Higher heat of fusion up to 259 kJ/kg [3] Available in wider range of melting points (-5 °C to 75.9 °C) [3] Lower thermal conductivity (0.25 W/m·K) [42] No corrosion [134] No toxicity [3] Low vapor pressure in molten state [3] Medium density up to 930 kg/m^3 [135] Cost economic with maximum \$4 per kg for technical grade [39] Commercially available at larger scales [136] Higher wetting ability [137] Chemically inert under 500 °C; above this temperature complex reactions occur such as cracking, aromatization, dehydrogenation etc. [4] No super cooling [4] Self-Nucleation [4]	Higher heat of fusion up to 259 kJ/kg [3] Available in wider range of melting points 7.8 °C to 127.2 °C [3] Low thermal conductivity to render insulating effect in building envelopes [116] No super-cooling [3] Solid–solid phase transition exists [79]	Higher heat of fusion up to 296 kJ/kg [3] Negligible volume change during phase change [138] Higher density (1640 kg/m^3 for T_m = 26.8 °C) [90] Very low cost, average \$0.17 per kg [93]	large volumetric latent heat due to strongest bonding [36] low vapor pressure [36] Small volume expansion during the phase transition [36] High boiling point (above 2000 °C) [36] Extremely large temperature gap between melting and boiling [36] No phase separation [36] Nonflammable [36]
Disadvantages	Flammable [134] Lower flash point (108 °C to 170 °C) for melting point 6 °C to 37 °C [56] Non-compatible with plastic container [3]	Some PCM are toxic [116] Mostly flammable [116] Most of them have low flash point and can be vulnerable to fire [116] Impurities greatly affect melting point [139] Produce harmful fumes [116] Unable to sustain high temperatures, oxidizing agents and flames [3] Some PCMs show corrosion after thermal cycling as shown in Table 4	Most of them show incongruent melting and lack of easy reversibility [2] Super cooling [140] Potentially corrosive to metals [138] Higher thermal conductivity in hot climates [112] Dehydration [141] Slightly toxic [3] Thermal conductivity (0.4–0.7 W/m·K) [142]	Highest thermal conductivity [36] Good electrical conductivity [36] Moderated super cooling [36] Might produce corrosion with building material but not experimented yet [36] High cost [36]

3. Methodologies of Microencapsulation of PCMs

There are several types of microencapsulation techniques, based on the underlying phenomena, which can be classified into three major categories: chemical processes, physico-chemical processes and mechanical processes. These methods are very common in medicine, food preservation, textile, cosmetic, agriculture, biotechnology, sensor industries, defense and engineering fields [143].

3.1. Chemical Processes

In chemical processes, a microcapsule wall is formed around the core material through chemical reactions. The processes consist of interfacial polymerization and in-situ polymerization, as explained in the following section.

3.1.1. Interfacial Polymerization

In interfacial polymerization, the solvent is selected to be non-reactive to the core material. The first monomer generates first polymers, which must be insoluble in the core material. Hence, the solution of the core material is prepared with this selected solvent. This solution is then spread all over the non-reactive medium (immiscible to this solution) and prepared as homogeneous droplets. A second monomer is added to this colloid with continuous stirring, which generates the first polymer. Before the generation of the first polymer, the second polymer wall is generated on the droplet. Continuous mild stirring causes the generation of first polymer wall inside the second polymer wall and, in doing this, a core material is micro-encapsulated inside a double-walled shell. This method of microencapsulation requires the first monomer to be composed of a minimum of two organic compounds (for instance two isocyanate groups and polypropylene glycol) [144]. Butyl stearate, as a core with the shell material of polyurea [145]; octadecane as a core with the shell material of polyurea [146]; di-ammonium hydrogen phosphate, as core with the shell material of polyurethane-urea [147]; xylitol, as a core with the shell material of polyuria-urethane [148]; butyl stearate, as a core with the shell material of polyurea/polyurethane [149]; *N*-octadecane, as a core with the shell material of polyurethane [150]; and *N*-octadecane, as a core with the shell material of polyurea [151], were successfully microencapsulated through this process. This process can yield microcapsules with a size range of 0.5–1000 µm [152] and its parameters are easy to control. The maximum temperature encountered is below 80 C which is considered much less hazardous than other methods [148]. However, the issue with this process is that bio-materials cannot be encapsulated using these materials [153]. The schematic diagram of the interfacial polymerization process for microencapsulation is shown in Figure 3, representing the various stages involved in the process [148].
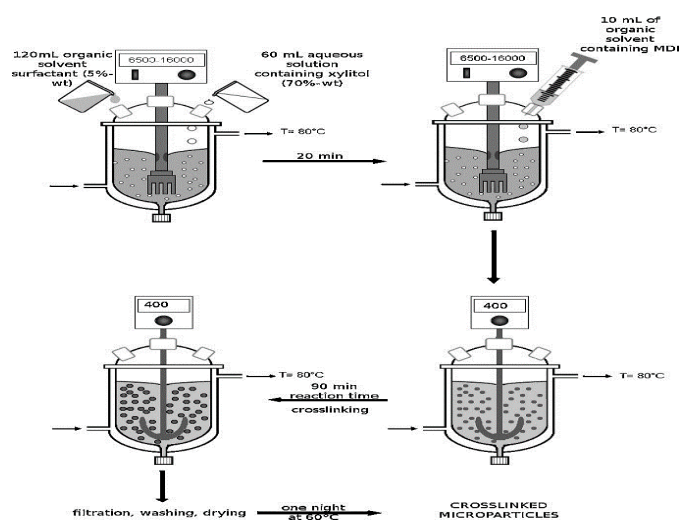

Figure 3. Schematic representation of the various stages of the microencapsulation process by the interfacial polycondensation method [148].

3.1.2. In-Situ Polymerization

In situ polymerization occurs in two stages. In the first stage, an aqueous polymer is added to the reactor along with distilled water at a certain temperature, followed by the addition of a cross-linking agent to the reactor. The mixture is stirred at high rotation (600 rpm) for 10 min followed by the addition of nucleating agents, resulting in a colloidal dispersion of the mixture. The pH of this mixture is adjusted to 3.5–4.0 with continuous stirring, followed by the addition of a calculated amount of coating to the dispersion. The reaction is carried out along with stirring, while gradually heating the dispersion up to 50 °C for a certain time. The suspension of formed capsules is cooled down, washed repeatedly, and eventually dried under controlled conditions. This method enables one to adjust the size of capsules, the size distribution and encapsulation ratio [154,155]. Paraffin wax, as a core material with urea formaldehyde as the shell material [59]; palmitic acid, as a core with aluminium oxyhydroxide (AlOOH) as the shell material [34]; hexadecane or octadecane, as a core with melamine-resin as the shell material [156]; higher hydrocarbons, as a core with amino-aldehyde resins as the shell material [157]; and *N*-hexadecane as a core with melamine–formaldehyde as the shell material, were encapsulated using this methodology. Through this process, capsules of a size range of 0.05–1100 μm [158–160] can be produced and it is capable of encapsulating many oil phase organic compounds [158]. Figure 4 represents the microencapsulation of essence oil by the process of in-situ polymerization [161].
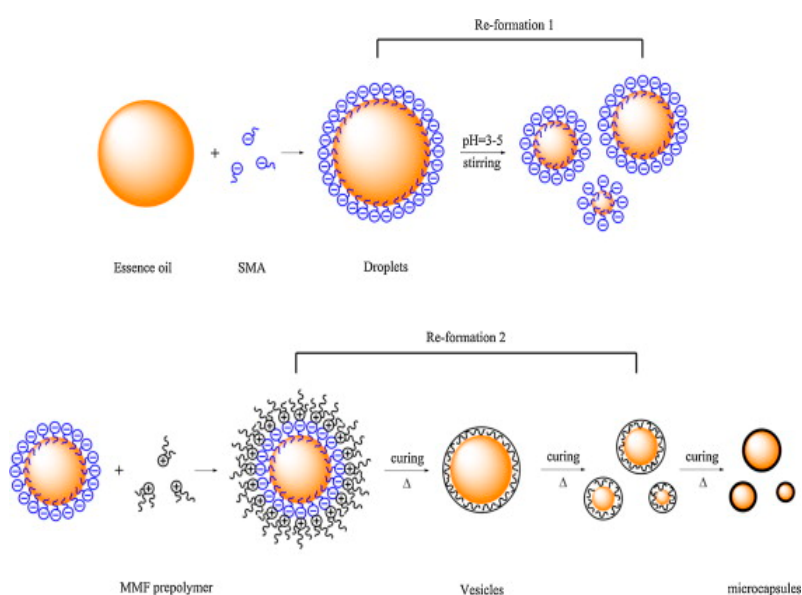

Figure 4. Schematics of the fabrication process of microcapsules containing essence oil by in situ polymerization [161].

3.2. Physico-Chemical Processes

These processes involve physical chemistry i.e., gelatin or coacervation yielding, forming stable and regular microspheres or microcapsules, which include coacervation and phase separation, sol–gel process, supercritical CO_2 assisted microencapsulation and solvent evaporation. Details of these processes are given in the following section.

3.2.1. Coacervation and Phase Separation

Fully solvated macromolecules are partially de-solvated in the macromolecular aggregation process. The difference between simple coacervation and complex coacervation is the method of phase separation. In simple coacervation, phase separation is induced by adding alcohol or salt, changing temperature or altering pH, while in complex coacervation, an oppositely charged polymer is

added to the polymer solution to form the coacervate phase by a cation–anion interaction [162]. Microencapsulation efficiency, via the coacervation method, is inversely proportional to the "core-to-coating ratio". It is obvious that smaller amounts of shell material may lead to an incomplete coating of PCM, which decreases its encapsulation efficiency, but increasing the proportion of shell material reduces the heat storage capacity of the microcapsules. The amount of cross-linking agent has a major role on encapsulation efficiency as it causes hardening of the shell due to the reaction of carboxylate with formaldehyde. Increasing the amount of agent increases its efficiency, but beyond a certain limit, efficiency decreases due to abundant amounts of the cross-linking agent that leads to inefficiency of the mechanism of the reaction. Similar is the case of emulsifying time where encapsulation efficiency increases with an increase in time, as it gives generation to droplets. However, if this homogenizing time is stretched beyond a certain limit of 10 min, then the phenomenon of coalesce occurs which reverses the solid into a liquid phase again [25]. Ammonium phosphate, as a core material, was encapsulated in different polymers by this method for fire retardation [163]. This process gives efficient control of the particle size [164]; simple coacervative is insensitive to water soluble additives and capable of the wide pH range in the system [165]. However, it is difficult to scale-up and it causes an agglomeration of Nano-particles [164]. Figure 5 shows the schematics of the equipment used for coacervation and phase separation process [166].
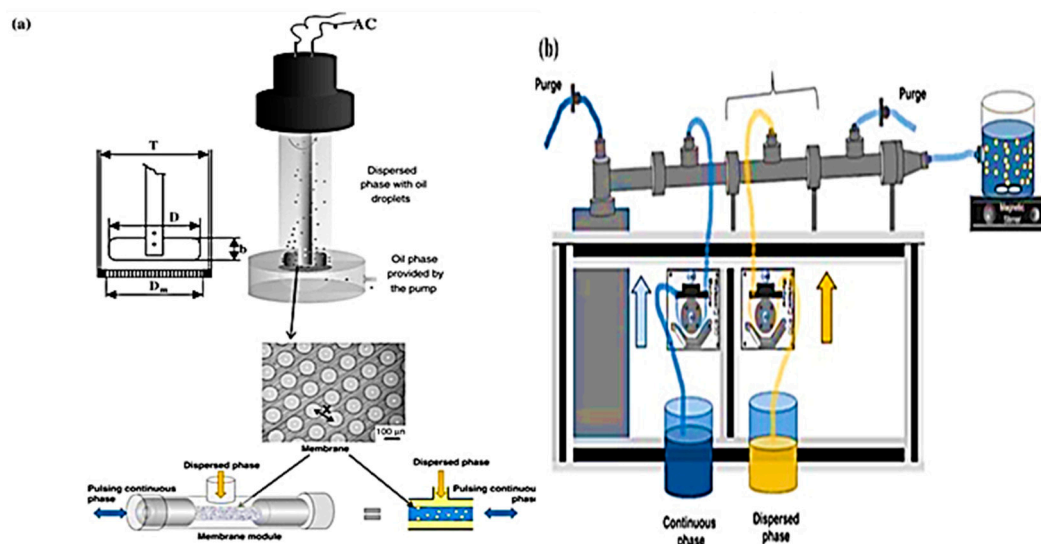

Figure 5. Illustration of experimental equipment for the generation of liquid drops using (**a**) dispersion cell with the simple paddle and (**b**) continuous pulsed phase flow [166].

This method was used to achieve stain free incorporation of PCM into encapsulated woven fabric to improve its thermal performance, however, minor leakage in two out of six samples was also reported [167]. The impact of time, the cross-linking agent, and mix ratio on the microencapsulation efficiency of the PCM, encapsulated by coacervation and the phase separation method, is investigated and these factors were in agreement with the above statements [25]. *N*-hexadecane, *N*-octadecane and *N*-nonadecane as a core material and gelatin and Arabic gum as the shell material [167]; paraffin oil as a core material with gelatin and Arabic gum as the shell material [168]; and *N*-octadecane as a core material with melamine-formaldehyde and styrene-maleic anhydride as the shell materials [169], used this method for microencapsulation.

3.2.2. Sol–Gel Encapsulation

In this method, an organic core material is dispersed in an aqueous solution to form droplets with the help of surfactants to obtain oil-in-water micro-emulsion. The sol–gel route starts with a

colloidal suspension, often more accurately a solution. In silica-based preparations, the commonly used tetraethoxysilane (TEOS) as a silica origin is dissolved in ethanol or a similar alcohol, hydrolyzed to silicic acid, and eventually condenses to form a silica gel network. Gelation of the sol is obtained through low-temperature hydrolysis and condensation reactions. The key to this method is the self-assembly of the silica precursor on the organic droplets under elaborate conditions, required for a reasonably rapid hydrolysis reaction to eventually form the silica shell [71]. TiO_2 as shell material is used to encapsulate paraffin by the sol–gel method and obtained good thermal stability and encapsulation efficiency [170]. Silica microsphere (hollow spheres) [171], monodisperse microspheres and gigantic hollow structures from silica shell material [172], and monodisperse microspheres with silica material [173] were prepared using this method. In this process, an inorganic shell with high thermal conductivity is formed around the capsule which is the disadvantage for building applications [164]. A schematic diagram of the encapsulation of *N*-octadecane core material with a silica shell is shown in Figure 6.
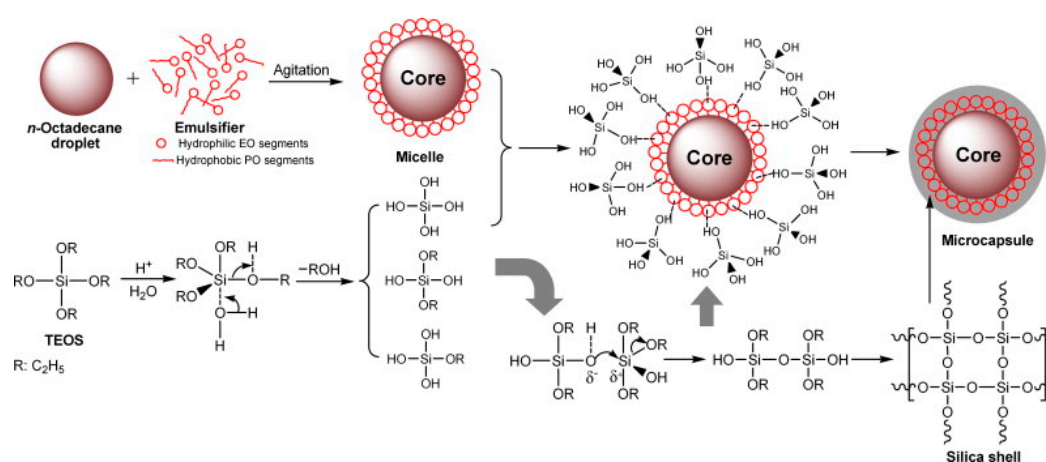

Figure 6. Schematic formation of the silica-microencapsulated *N*-octadecane via a sol–gel encapsulation [71].

3.2.3. Supercritical CO_2 Assisted Microencapsulation

This process is further divided into static and dynamic. The static version involves the pre-mixing of supercritical CO_2 and a solution containing a solute of interest at a pressure higher than the critical pressure of CO_2. After equilibrium is established, the mixture in a high-pressure chamber is allowed to expand to atmospheric pressure through a flow restrictor (or a capillary tube), by expansion into a drying chamber. The dynamic version involves continuous intimate mixing of a solution containing a solute of interest and supercritical CO_2 or near-critical CO_2. The two fluid streams become intimately mixed in a low, dead volume, subsequently expanded through a flow restrictor to atmospheric pressure, where the micro-droplets are rapidly dried [174]. The schematics of this process are shown in Figure 7. Generally, this technology is used for the encapsulation of biomaterials and medicines. Piroxicam (drug) as a core material with the poly lactic acid and poly lactic-*co*-glycolic acid as the shell material [175]; and proteins and bovine serum albumin as a core material with liposome as the shell material [176] were microencapsulated through this process. The literature on microencapsulating starch using this method is compiled in [177]. The advantages of this process are low critical temperature value, nontoxic, nonflammable, cost effective and readily available [178] but it is still in the research phase [153].
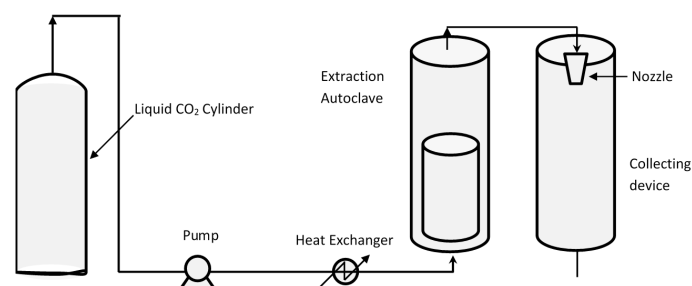
Figure 7. Schematic flow diagram of the supercritical CO_2 assisted microencapsulation process [179].

3.2.4. Solvent Evaporation

Oil in water emulsion is produced by the agitation of two immiscible liquids in the solvent evaporation encapsulation method. Microcapsule shell material (polymer) is dissolved in a volatile solvent, immiscible with the emulsion, followed by the dissolution or dispersion of core material in the coating polymer solution. The core-coating material mixture is dispersed with agitation in the emulsion to obtain appropriately sized microcapsules. Agitation of the system is continued until the solvent partition and water contents are removed by evaporation. Several methods can be used to achieve dispersion of the oil phase in the continuous phase summarized in [180]; a schematic representation of this process is represented in Figure 8 [181]. Generally, this encapsulation method is adapted in the pharmaceutical industry. Bovine serum albumin as a core with poly(DL-lactide-*co*-glycolide) as the shell material [182]; proteins and peptides as a core with poly(lactic acid) and poly(lactic-*co*-glycolic acid) as the shell material [181]; verapamil and propranolol as a core with Eudragit RS and Eudragit RL polymers as the shell material [183], were encapsulated using this process. This process is economical but restricted to lab scale production [164] and constrained to the pharmaceutical industry only [181–183].
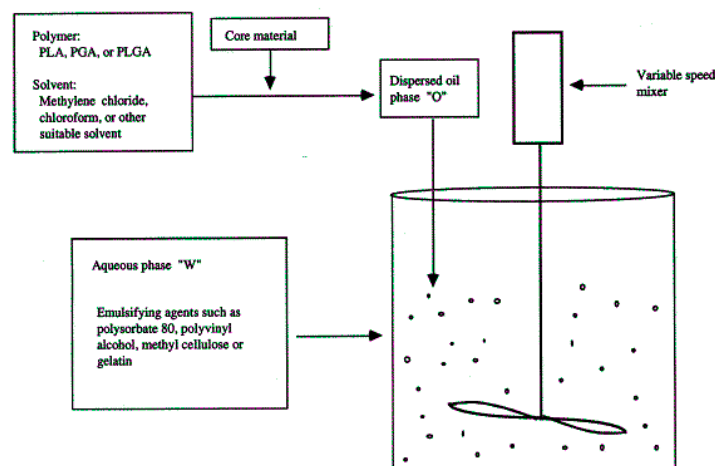

Figure 8. Schematic diagram of the oil in water (O/W) emulsion solvent evaporation method [181].

3.3. Mechanical Processes

In these processes, the coating is carried out around core material through some mechanical process. These processes are spray drying and congealing, fluid bed coating, multi-orifice centrifugal process, air suspension coating and pan coating as explained below.

3.3.1. Spray Drying and Congealing

Spray drying is a physical method used for microencapsulation of PCMs. A chamber is used for spraying in which some inert gas (air or nitrogen gas) is kept. The inside temperature is adjusted so that it can cause evaporation of the solvent and can formulate encapsulated PCM in

solid form. Thermoplastics are used here as the shell material. A solution is prepared containing a core material, encapsulating agent and a medium that can accommodate the homogenous mixture of these components in the liquid phase. An atomizer is used to spray small proportions of emulsion into the chamber with set conditions of temperature and inert gas. That gas will evaporate the solvent and condense to form solid capsules. In the following step, these solid capsules are separated by using a filter or cyclones. The solvent can be condensed by some means to reuse it for the next encapsulation [184]. Paraffin as a core material and gelatin and acacia as the shell material [25]; paraffin RT27 as a core material with polyethylene/ethylene vinyl acetate as the shell material [185], were used for microencapsulation through this process. This method is reviewed to produce Nano-particles electronic and optoelectronic, mechanical, chemical, cosmetic, medical, drug, and food technologies [186]. This process is cost economic and commercial [152], equipment and knowledge are widely available [153,164], it is versatile for many materials [153,164] and easy to scale-up [153]. Its disadvantages are high process temperature, the agglomeration of particles, and incomplete coating [164]. Figure 9 shows the schematic diagram of the spray drying process.
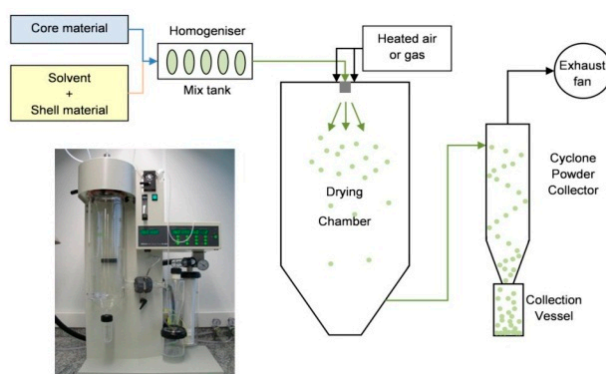

Figure 9. Schematic diagram of the spray drying process [187].

3.3.2. Fluid Bed Coating

This method of encapsulation is basically a coating process in which droplets of coating material solution are atomized through a nozzle into a hot gas, fluidized particle bed. After the atomized droplets of the coating material come into contact with core particles, the solvent has to evaporate quickly. An excess of droplets in the bed would induce agglomeration, therefore, appropriate droplet atomizing and drying conditions are maintained to eliminate agglomeration of solid particles. Usually, this is formed for fine particles (Ø <70 μm) due to their strong cohesive forces. So this method cannot be used for fine particles using the conventional fluid bed process [162]. Bischofite as a core material and acrylic polymer as the shell material [188], and foods as the core material [189] were encapsulated through this process. Literature related to fluid bed coating to encapsulate food items is reviewed in [190]. Top-spray coater and bottom-spray coater, being most popular in the fluid bed coating process, are shown in Figure 10.

3.3.3. Multi Orifice Centrifugal Process

In this process, core material particles are accelerated through an encapsulant membrane with the help of centrifugal force yielding microcapsules. This process is capable of producing microcapsules with solid and liquid core materials, different shell materials and of different sizes. These outputs depend on the parameters of the rotational speed of the cylinder, the flow rate of the core and shell material, concentration, viscosity and surface tension of the core material. The production rate of the process is 50 to 75 pounds per hour [180]. The production rate is comparable or even higher than that of regular spray drying or spray cooling processes and the processing cost is also very similar. It involves a high process temperature and creates clogging problems [191]. It is suitable for bio-encapsulation [164].
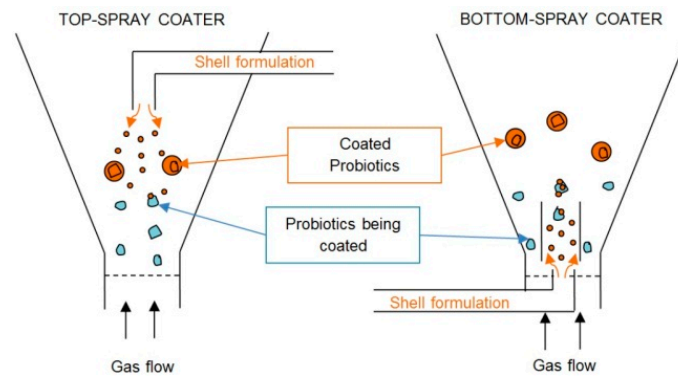
Figure 10. Schematic diagrams of two types of the most commonly used fluid bed coaters [187].

3.3.4. Air Suspension Coating

In air suspension coating, the core material is dispersed in the upward air stream that is supporting the suspended solid particles. In this upward air chamber, the shell material is sprayed onto the suspended particles and the air is circulated again in order to achieve the required thickness of the coating, along with drying the capsules [180]. This complex process, with almost 20 parameters, is generally applied in the pharmaceutical industry [192]. Micro-processes (drying, droplet impact and spreading, and stickiness) are identified [193], which play a vital role in the efficiency of this method. This process is cost economic and gives higher production volume [164]. The necessity of a high skill level, being unsuitable to encapsulate PCM [194], applicable only to solid cores [195] and substantially non-uniform capsules [196] are shortcomings of this process. Figure 11 represents the schematic diagram of this process.
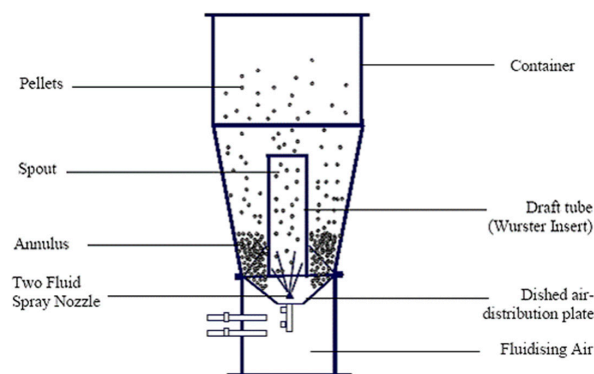

Figure 11. Schematic diagram of air suspension coating [197].

3.3.5. Pan Coating

Pan coating is used for capsules of greater size (Ø >600 μm), and is often used for the encapsulation of controlled release beads and pills in the pharmaceutical industry [194]. Shell material in the form of a solution or atomized spray is coated over the solid core material. Later, warm air or a drying oven is used to remove the coating solvent [180]. Using this method, the mixing of tablets is investigated by altering parameters of rotation speed and rotation cycles and the results are validated by using the discrete element model [198], and another study evaluated that pan coating can be applied uniformly to the capsules [199]. This process is used in the pharmaceutical industry for pills [194] and in the food industry for candies [200]. It is time-consuming [195], not suitable to encapsulate PCM [194] and yields substantially non-uniform coating [196].

All the processes are reviewed from the perspectives of manufacturing parameters, economics, and suitability for different categories of core and shell materials and their comparison is drawn in Table 10.

Table 10. Comparison of different microencapsulation techniques.

	Chemical Processes		Physio–Chemical Processes					Mechanical Processes			
	Interfacial Polymerization	In-Situ Polymerization	Coacervation and Phase Separation	Sol–Gel Encapsulation	Supercritical CO_2	Solvent Evaporation	Spray Drying and Congealing	Fluid Bed Coating	Micro-Orifice—Centrifugal Process	Air-Suspension Coating	Pan Coating
Merits	Size range (0.5–1000 μm) [152] Easy control parameters [148] System temperature up to 80 °C [148]	Size range (0.05–1100 μm) [158–160] Capable of encapsulating many oil phase organic compounds [158] System temperature up to 80 °C [201]	Size range (2–1200 μm) [152] Versatile [164] Efficient control of the particle size [164] Simple coacervative is insensitive to water soluble additives [165] Simple coacervative is capable of wide pH range in the system [165]	Size range (0.2–20 μm) [202]	Low critical temperature value Nontoxic Nonflammable [178] Readily available [178] Highly pure [177] Cost effective [178] Can produce Nano-capsules [178] Replacement of organic solvents [153]	Size range (0.5–1000 μm) [152] Low cost [164]	size range (5–5000 μm) [152] Low-cost commercial process [152] Equipment and know—how widely available [153,164] Versatile [152,163] Easy to scale-up [153]	Size range (20–1500 μm) [152]	Size range (5–1500 μm) [152]	Low-cost [164] Higher production volume [164]	Size range (600–5000 μm) [152] Low cost equipment [153,164] Used in pharmaceutical industry for pills [194] and in food industry for candies [200]
Demerits	Non-biocompatible career material Organic solvents [153]	NA	Aldehyde as hardener being toxic [164] Difficult to scale-up [164] Agglomeration of Nano-particles [164] Necessity of complete salt removal from encapsulated product [165]	Inorganic shell with high thermal conductivity as non-insulator for building applications [164]	Still under research [153]	Restricted to lab scale production [164] Restricted to pharmaceutical industry only [182,183]	High temperature Agglomeration of particles Remaining uncoated [163]	NA	High temperature [164] Suitable for bio-encapsulation [164] Clogging problems [191]	High skill level required [164] Not suitable to encapsulate PCM [194] Applied only to solid cores [195] Agglomeration of particles [164] Substantially non-uniform [196] Complex process involving nearly 20 variables [192]	Difficult to control High skill level required [153,163] Not suitable to encapsulate PCM [194] Substantially non-uniform coating [196] Time-consuming [195] Inconsistent encapsulation efficiency [195]

4. Performance of Microencapsulated PCMs in Buildings

4.1. Modelling Studies

Most of the numerical models focus on PCM wall optimization that includes PCM wall thickness, placement of a PCM layer inside the wall, phase transition temperature and heat storage capacity of the materials. Heat conductivity of the material and wall thickness play vital roles in the completion of the charging–discharging cycle over a 24 h period. Optimal thickness will depend on the thermal conductivity of the material. These models ignore the effect of convective heat transfer within the melted PCM. In the following section, numerical models are surveyed with regard to PCM in building applications.

Effective thermal conductivity of mono-disperse and poly-disperse encapsulated particles, randomly or uniformly distributed inside a matrix, was predicted. It is reported that effective thermal conductivity has no effect on capsule size and spatial distribution, however; volume fraction of core and shell and thermal conductivities of the core, shell, and matrix do influence the effective thermal conductivity [203]. Darkwa presented that the heat transfer rate depends on the spatial distribution of the PCM particles inside building components and this rate is more in triangular particles as compared to square ones [204]. Zhou et al. adopted a one-dimensional enthalpy model, using a fully implicit finite difference scheme to demonstrate thermal performance of PCM in wallboards and reported that above critical values of latent heat of fusion and thickness of PCM layers inside wallboard have very little impact on damping and delay of temperature peaks [205].

A uni-directional heat transfer model was developed using a finite volume scheme to predict the performance of roof comprising of PCM, concrete and steel, considering concrete slab and roof top, independent of temperature. It showed that the daytime inner surface temperature for PCM is low as compared to a non-PCM ceiling due to higher thermal inertia, while it was opposite in the nighttime due to the heat energy stored in the PCM [206]. An inverse method was applied to solve numerical modeling and assumed the conductivity of all materials involved to be constant to validate the experimental results. The results concluded that a 5 mm of PCM layer board had twice the thermal inertia of non-PCM wallboard and performed equivalently to an 8 cm thick concrete wall [207]. A finite element algorithm validated the prototype experimental results that an air layer between PCM and metal in the wallboard can enhance thermal mass sensibly, with ease of installation [208].

The incorporation of PCM filled cylindrical holes, created inside bricks, was numerically studied for cooling potential in hot climates through the finite element method. The two-dimensional heat flow was analyzed, neglecting thermal expansion of brick containing PCM and natural convection of PCM in the liquid phase [209]. It was reported that the effect of natural convection in liquid regime is significant where Raleigh Number (R_a) is greater than 5×10^6 while insignificant when R_a is below 1×10^6 [210]. It is proved numerically that laminated PCM wallboards are better than randomly distributed PCM wallboards in terms of enhanced thermal performance and rapid heat transfer rate [211]. A validated numerical model predicted the performance of a form-stable PCM, thereby proposing optimum transition temperatures, thermal conductivity, and acceptable mechanical properties [212]. The inclusion of PCM (paraffin) as an ingredient to self-compacting concrete was modeled and its effect on hydration temperature of the concrete was studied [213]. It was observed that the inclusion of PCM substantially lowered the hydration temperature and thermal conductivity, however, the compressive strength was reported to decrease by up to 71% with the inclusion of PCM, by a 5% weight ratio within 28 days of exposure [213]. A heat transfer model predicted that laminated wallboards exhibit a higher heat storage capacity compared to randomly distributed wallboards [214]. It was predicted that PCM performance is strongly dependent on the thickness of the walls, phase change temperature, and total latent heat of the PCM [215], crucial to enhance thermal inertia of the buildings [216]. Phase changing component materials are better than ordinary masonry wall for energy efficiency and thermal comfort [217], especially those with sharp melting points [218].

4.2. Experimental Studies

Drissi et al. carried out the experimental characterization using differential scanning calorimetry (DSC) to study the damage in the microencapsulated PCM (powder Micronal® DS 5038X from BASF encapsulated in polymethyl methacrylate shell) and reported that a damaged PCM can lose 28% of latent heat compared to non-damaged PCM [219]. Stearic acid (SA) is used as a PCM and its composite, with titanium dioxide (TiO_2), is prepared [76]. No chemical reaction occurred during its formation. It is non-flammable, non-toxic and thermally stable but its thermal storage capacity is low i.e., 46.6 kJ/kg. Table 11 contains the summary of different types of PCMs integrated into building components and their thermal performance is tabulated.

Table 11. Summary of the PCM performance in the buildings.

Study	PCM Material/Product	Building Component	Performance
Experimental + Numerical [206]	$CaCl_2$ + NaCl + KCl + H_2O	Roof	Diurnal ceiling temperature range of 6 °C without PCM was reduced to 1 °C using PCM.
Experimental + Numerical [207]	DuPont wallboard	Walls	5 mm of the PCM wallboard can increase the thermal inertia equivalent to 8 cm thick concrete layer.
Experimental + Numerical [208]	Eutectic salts	Sandwich panels	Air layer between PCM and metal in the wallboard can enhance thermal mass sensibly.
Numerical [209]	*N*-Octadecane, *N*-Eicosane, P116	PCM filled in bricks	Heat flux at the indoor space can be reduced by 17.55% at maximum.
Numerical [211]	NA	Wallboard	Laminated PCM wallboards are better than randomly distributed PCM wallboards in terms of enhanced thermal performance and rapid heat transfer rate.
Experimental [214]	Micronal DS 5008 X	Concrete	PCM lowered the hydration temperature and the compressive strength was decreased up to 71% with inclusion of PCM by 5% weight ratio within 28 days of exposure
Numerical [215]	PCM–gypsum composite	NA	PCM performance is strongly dependent on thickness of the wall, phase change temperature, and total latent heat of the PCM.
Numerical [217]	NA	Wall	PCM wall is preferred over ordinary masonry wall in terms of efficient thermal energy storage.
Numerical [218]	PCM–gypsum	Walls + ceiling	2 different PCMs were compared in the specific climatic conditions and 1 performed better than the other.
Experimental + Numerical [220]	PCM-enhanced fiber insulation	Wall assembly	Time shift of 3 h with 20%–35% peak hour load reduction is achieved by using PCM.
Experimental [221]	Cellulose-PCM Blend	NA	Cellulose insulation containing 22% of PCM reduced 40% of the surface heat flow.
Experimental + Numerical [222]	ThermoMax	TABS and PCM in prefabricated concrete deck element	The cooling performance of thermally activated building system (TABS) was reduced with the integration of PCM.
Experimental + Numerical [223]	Paraffin RT-21	Prefabricated concrete slab filled with PCM tubes	It reduced 66% of the cooling load in hot weather and eliminated active cooling system in mild summer. The energy saving was 45% in mild winter and 21% in severe winter.

Bio-based PCM is microencapsulated with fiber insulations for thermal regulations. Kosny et al. worked on fiber insulations containing microencapsulated PCM, numerically and experimentally. They have justified the use of a blend in terms of peak load shifting and energy optimization. The PCM achieved a time shift of three hours, with a 20%–35% peak hour load reduction being achieved [220].

In different studies, PCM-cellulose blends are investigated for the thermal insulation of buildings to keep room temperature independent of outside temperature fluctuations. It is obvious that the addition of PCM can insulate a building more efficiently. This study focused on the optimal quantity of PCM inside insulator fibers with constant thermal conductivity. The PCM, blended with fiber, increased thermal inertia of the building while increasing the PCM melting time to 15 h [62,221].

Pomianowski et al. introduced the concept of PCM and thermally activated building system (TABS) jointly for cooling buildings. In this study, they carried out simulations and experimental

work to validate numerical predictions for PCM impact on the thermal performance of the building. They reported major discrepancies between theoretical and experimental results and cooling performance of TABS reduced when PCM was added to it [222]. Navarro et al. also experimented on the inclusion of macro encapsulated PCM inside TABS and tried to cover the heating and cooling of a building during winter and summer seasons. Simulations were conducted for hot, mild, and cold weather conditions. This system was capable of providing 66% of the cooling demand in hot weather and eliminated the mechanical cooling system in mild weather. The energy saving was 45% in mild winter and 21% in severe winter [223].

5. Problems of Microencapsulation

Microencapsulated *N*-octadecane PCM in a sodium silicate shell was prepared by the sol–gel method. Spherical microcapsules with a specified chemical composition were successfully fabricated. After integration to concrete blocks, PCM release was reported, reaching up to 40% in 30 days of exposure, which undermined the reliability of the method over long-time building integration. Additionally, it was observed that using a larger shell to core ratio, to ensure effective encapsulation, resulted in a 59% loss of energy storage capacity of PCM [72]. The method was improved with slight modifications, resulting in better microencapsulation efficiency (86.5%) and a better encapsulation ratio (86%), however, thermal instability was observed at elevated temperatures (releasing 20% PCM at 250 °C reaching up to 100% at 500 °C). This sharp weight loss with an increase in temperature raises the safety concerns in case the building catches fire [71].

In another study, *N*-octadecane PCM was encapsulated in calcium carbonate, achieving up to 40% microencapsulation efficiency with up to 40% microencapsulation ratio. However, up to a 23% loss of PCM was reported in 30 days of exposure in a temperature range of 160 °C to 250 °C [58]. Wolcott blended paraffin with polymers and investigated their behavior for thermal energy storage. Although this blend did not considerably affect the crystallinity and melting temperature of PCM, however up to 10% of paraffin PCM leaked within 40 h of exposure at 60 °C [70]. Caprylic acid as PCMs was encapsulated in different shell materials by opting for simple and complex coacervation techniques, concluding that emulsion temperature and stirring time were major factors affecting micro-encapsulation efficiency [78].

Salt hydrate was microencapsulated in the polymer shell by the suspension copolymerization-solvent volatile method. An improved thermal cycling through modification in its chemical composition was reported. However, incongruent melting was observed due to a change in the number of water molecules with the fluctuation of temperature yielding different melting points. The incongruence can be attributed to dehydration of the hydrated salts (observed by weight loss) with an increase in temperature [115]. In order to achieve integrity in salt hydrates, salts were micro-encapsulated by the solution impregnation method in expanded graphite. The micro-encapsulation resulted in a six-fold increase in encapsulation efficiency and a thermal stability of up to 100 cycles [114].

A eutectic mixture of fatty acids was tested for passive cooling of buildings which shows structural integrity of up to 120 °C, however, the addition of only 2% PCM in concrete reduced its compressive strength by 30% [35]. Nano-graphite (NG) was added to paraffin wax to produce a composite material and its thermal conductivity was investigated. Paraffin was immersed in expanded graphite and was studied numerically and experimentally for melting and solidification behavior of the composite. It was reported that thermal conductivity enhanced greatly with the formation of flake structures. However, the leakage of PCM was observed after exposure, thereby asking for an improvement in PCM micro-encapsulation to avoid leakage [68].

6. Conclusions and Recommendation

In the article, the research on microencapsulated PCMs for thermal energy storage in buildings is reviewed, focusing on thermal, structural and environmental aspects. It is observed that paraffins are

preferred due to self-nucleating properties, the absence of sub-cooling and congruent melting, higher latent heat of fusion and the availability in a wide range of melting points suitable for many applications. Its lower thermal conductivity can be exploited for building applications, creating an insulating effect. Most of the microencapsulation techniques yield fine capsules with good microencapsulation efficiency. When integrating PCM into a concrete, temperature rise, due to hydration, causes PCM leakage which hinders the movement of water that ultimately reduces the compressive strength of concrete.

Core to coating ratio is a major optimization parameter that affects microencapsulation efficiency. Increasing the amount of coating material increases microencapsulation efficiency but, in turn, reduces heat storage capacity. On the other hand, decreasing the amount of coating results in reduced strength of micro-encapsulated PCMs.

Furthermore, the presence of PCM Microcapsules affects the mechanical strength of the building structure. Increasing the amount of PCM in construction materials can increase thermal inertia of the building however, simultaneously, it reduces its compressive strength considerably. Encapsulant materials that offer a strong and durable shell around PCM and provide good bonding with the construction material, i.e., concrete, need to be investigated. In the context of encapsulant materials, metal oxides are studied to improve mechanical strength, however, they need further attention for improvement in terms of environmental corrosion. Low melting point metals have a huge latent heat of fusion and better thermal stability for millions of charging–discharging cycles and can be potential PCMs for building applications.

The thermal models predicting PCM behavior in building components need to be improved to address natural convection within PCM, sub-cooling, super cooling and dehydration in certain materials. In addition, the application of microencapsulated PCMs is not widely tested in various climatic conditions, with various heat loads, to determine their long-term structural and thermal stability, which is a potential area of future research.

Author Contributions: The paper is a joint work where Ahmad Hasan provided the write up material, Yasir Rashid prepared the first draft, Ahmad Hasan and Shakeel Laghari reviewed the manuscript and Yasir Rashid prepared the final draft.

Conflicts of Interest: The authors declare no conflict of interest.

Abbreviation

Ø	Diameter
CNFs	Carbon Nano-fibers
DSC	Differential scanning calorimetry
EG	Expanded graphite
GNPs	Graphene Nano-platelets
HDPE	High-density polyethylene
ΔH	Latent heat
L-MWCNTs	Long multi-walled carbon Nano Tubes
LDPE	Low-density polyethylene
LLDPE	Linear low-density polyethylene
T_m	Melting temperature
μm	Micro meter
MePCMs	Microencapsulated phase change materials
NA	Information not available
NG	Nano graphite
PCM	Phase change material
PS	Polystyrene
R_a	Rayleigh number
S-MWCNTs	Short multi-walled carbon Nano-Tubes

C_p	Specific heat capacity
TABS	Thermally activated building system

References

1. Kuznik, F.; Virgone, J.; Noel, J. Optimization of a phase change material wallboard for building use. *Appl. Therm. Eng.* **2008**, *28*, 1291–1298. [CrossRef]

2. Farid, M.M.; Khudhair, A.M.; Razack, S.A.K.; Al-Hallaj, S. A review on phase change energy storage: Materials and applications. *Energy Convers. Manag.* **2004**, *45*, 1597–1615. [CrossRef]

3. Sharma, A.; Tyagi, V.V.; Chen, C.R.; Buddhi, D. Review on thermal energy storage with phase change materials and applications. *Renew. Sustain. Energy Rev.* **2009**, *13*, 318–345. [CrossRef]

4. Kuznik, F.; David, D.; Johannes, K.; Roux, J.J. A review on phase change materials integrated in building walls. *Renew. Sustain. Energy Rev.* **2011**, *15*, 379–391. [CrossRef]

5. Zalba, B.; Marín, J.M.; Cabeza, L.F.; Mehling, H. Review on thermal energy storage with phase change: Materials, heat transfer analysis and applications. *Appl. Therm. Eng.* **2003**, *23*, 251–283. [CrossRef]

6. Zhou, D.; Zhao, C.Y.; Tian, Y. Review on thermal energy storage with phase change materials (PCMs) in building applications. *Appl. Energy* **2012**, *92*, 593–605. [CrossRef]

7. Liu, L.; Su, D.; Tang, Y.; Fang, G. Thermal conductivity enhancement of phase change materials for thermal energy storage: A review. *Renew. Sustain. Energy Rev.* **2016**, *62*, 305–317. [CrossRef]

8. Da Cunha, J.P.; Eames, P. Thermal energy storage for low and medium temperature applications using phase change materials—A review. *Appl. Energy* **2016**, *177*, 227–238. [CrossRef]

9. Jurkowska, M.; Szczygieł, I. Review on properties of microencapsulated phase change materials slurries (mPCMS). *Appl. Therm. Eng.* **2016**, *98*, 365–373. [CrossRef]

10. Akeiber, H.; Nejat, P.; Majid, M.Z.A.; Wahid, M.A.; Jomehzadeh, F.; Famileh, I.Z.; Zaki, S.A. A review on phase change material (PCM) for sustainable passive cooling in building envelopes. *Renew. Sustain. Energy Rev.* **2016**, *60*, 1470–1497. [CrossRef]

11. Kylili, A.; Fokaides, P.A. Life Cycle Assessment (LCA) of Phase Change Materials (PCMs) for building applications: A review. *J. Build. Eng.* **2016**, *6*, 133–143. [CrossRef]

12. Zhang, P.; Xiao, X.; Ma, Z.W. A review of the composite phase change materials: Fabrication, characterization, mathematical modeling and application to performance enhancement. *Appl. Energy* **2016**, *165*, 472–510. [CrossRef]

13. Silva, T.; Vicente, R.; Rodrigues, F. Literature review on the use of phase change materials in glazing and shading solutions. *Renew. Sustain. Energy Rev.* **2016**, *53*, 515–535. [CrossRef]

14. Bédécarrats, J.P.; Castaing-Lasvignottes, J.; Strub, F.; Dumas, J.P. Study of a phase change energy storage using spherical capsules. Part I: Experimental results. *Energy Convers. Manag.* **2009**, *50*, 2527–2536.

15. Zhou, G.; Yang, Y.; Xu, H. Energy performance of a hybrid space-cooling system in an office building using SSPCM thermal storage and night ventilation. *Sol. Energy* **2011**, *85*, 477–485. [CrossRef]

16. Mehling, H.; Schossig, P.; Kalz, D. *Latent Heat Storage in Buildings*; FIZ Karlsruhe GmbH: Eggenstein-Leopoldshafen, Germany, 2009.

17. Yen, T.; Chen, H.J.; Huang, Y.L.; Ko, C.T. The dividing strength of lightweight aggregate concrete and the packing strength of light-weight aggregate. *J. Chin. Inst. Eng.* **1998**, *21*, 611–618. [CrossRef]

18. Sarı, A.; Karaipekli, A.; Alkan, C. Preparation, characterization and thermal properties of lauric acid/expanded perlite as novel form-stable composite phase change material. *Chem. Eng. J.* **2009**, *155*, 899–904. [CrossRef]

19. Khosrojerdi, M.; Mortazavi, S.M. Impregnation of a porous material with a PCM on a cotton fabric and the effect of vacuum on thermo-regulating textiles. *J. Therm. Anal. Calorim.* **2013**, *114*, 1111–1119. [CrossRef]

20. Ingole, P.R.; Mohod, T.R.; Gaddamwar, S.S. Use of Phase Change Materials in Construction of Buildings: A Review. *Int. J. Eng. Res. Gen. Sci.* **2014**, *2*, 624–628.

21. Cabeza, L.F.; Castellon, C.; Nogues, M.; Medrano, M.; Leppers, R.; Zubillaga, O. Use of microencapsulated PCM in concrete walls for energy savings. *Energy Build.* **2007**, *39*, 113–119. [CrossRef]

22. Wang, X.; Zhang, Y.; Xiao, W.; Zeng, R.; Zhang, Q.; Di, H. Review on thermal performance of phase change energy storage building envelope. *Chin. Sci. Bull.* **2009**, *54*, 920–928. [CrossRef]

23. Cabeza, L.F.; Roca, J.; Noguees, M.; Mehling, H.; Hiebler, S. Long term immersion corrosion tests on metal-PCM pairs used for latent heat storage in the 24 to 29° C temperature range. *Mater. Corros.* **2005**, *56*, 33–39. [CrossRef]

24. Jacob, R.; Bruno, F. Review on shell materials used in the encapsulation of phase change materials for high temperature thermal energy storage. *Renew. Sustain. Energy Rev.* **2015**, *48*, 79–87. [CrossRef]

25. Hawlader, M.N.A.; Uddin, M.S.; Khin, M.M. Microencapsulated PCM thermal-energy storage system. *Appl. Energy* **2003**, *74*, 195–202. [CrossRef]

26. Dubey, R. Microencapsulation technology and applications. *Def. Sci. J.* **2009**, *59*, 82–95.

27. Lam, P.L.; Gambari, R.; Kok, S.L.; Lam, K.H.; Tang, J.O.; Bian, Z.X.; Chui, C.H. Non-toxic agarose/gelatin-based microencapsulation system containing gallic acid for antifungal application. *Int. J. Mol. Med.* **2015**, *35*, 503–510. [CrossRef] [PubMed]

28. Salazar-López, E.I.; Jiménez, M.; Salazar, R.; Azuara, E. Incorporation of microcapsules in pineapple intercellular tissue using osmotic dehydration and microencapsulation method. *Food Bioprocess Technol.* **2015**, *8*, 1699–1706. [CrossRef]

29. Sarı, A.; Alkan, C.; Döğüşcü, D.K.; Kızıl, Ç. Micro/nano encapsulated *N*-tetracosane and *N*-octadecane eutectic mixture with polystyrene shell for low-temperature latent heat thermal energy storage applications. *Sol. Energy* **2015**, *115*, 195–203. [CrossRef]

30. Butstraen, C.; Salaün, F.; Devaux, E. Sol–gel microencapsulation of oil phase with Pickering and nonionic surfactant based emulsions. *Powder Technol.* **2015**, *284*, 237–244. [CrossRef]

31. Carvalho, I.T.; Estevinho, B.N.; Santos, L. Application of microencapsulated essential oils in cosmetic and personal healthcare products—A review. *Int. J. Cosmet. Sci.* **2016**, *38*, 109–119. [CrossRef] [PubMed]

32. Mahdavi, S.A.; Jafari, S.M.; Assadpoor, E.; Dehnad, D. Microencapsulation optimization of natural anthocyanins with maltodextrin, gum Arabic and gelatin. *Int. J. Biol. Macromol.* **2016**, *85*, 379–385. [CrossRef] [PubMed]

33. Sarı, A.; Alkan, C.; Karaipekli, A.; Uzun, O. Microencapsulated *N*-octacosane as phase change material for thermal energy storage. *Sol. Energy* **2009**, *83*, 1757–1763. [CrossRef]

34. Pan, L.; Tao, Q.; Zhang, S.; Wang, S.; Zhang, J.; Wang, S.; Zhang, Z. Preparation, characterization and thermal properties of micro-encapsulated phase change materials. *Sol. Energy Mater. Sol. Cells* **2012**, *98*, 66–70. [CrossRef]

35. Cellat, K.; Beyhan, B.; Güngör, C.; Konuklu, Y.; Karahan, O.; Dündar, C.; Paksoy, H. Thermal enhancement of concrete by adding bio-based fatty acids as phase change materials. *Energy Build.* **2015**, *106*, 156–163. [CrossRef]

36. Ge, H.; Li, H.; Mei, S.; Liu, J. Low melting point liquid metal as a new class of phase change material: An emerging frontier in energy area. *Renew. Sustain. Energy Rev.* **2013**, *21*, 331–346. [CrossRef]

37. Konuklu, Y.; Ostry, M.; Paksoy, H.O.; Charvat, P. Review on using microencapsulated phase change materials (PCM) in building applications. *Energy Build.* **2015**, *106*, 134–155. [CrossRef]

38. Nkwetta, D.N.; Haghighat, F. Thermal energy storage with phase change material—A state-of-the art review. *Sustain. Cities Soc.* **2014**, *10*, 87–100. [CrossRef]

39. The Candle Making Shop. Available online: http://www.thecandlemakingshop.co.uk/Candle-Wax/Bulk-Waxes/pure-paraffin-wax-20kg.aspx (accessed on 21 December 2015).

40. Anghel, E.M.; Georgiev, A.; Petrescu, S.; Popov, R.; Constantinescu, M. Thermo-physical characterization of some paraffins used as phase change materials for thermal energy storage. *J. Therm. Anal. Calorim.* **2014**, *117*, 557–566. [CrossRef]

41. Kośny, J. Short History of PCM Applications in Building Envelopes. In *PCM-Enhanced Building Components*; Springer International Publishing: Basel, Switzerland, 2015; pp. 21–59.

42. The Engineering ToolBox. Available online: http://www.engineeringtoolbox.com/thermal-conductivity-d_429.html (accessed on 25 February 2016).

43. Hough, T.P. *Solar Energy: New Research*; Nova Publishers: New York, NY, USA, 2006.

44. Mehrali, M.; Latibari, S.T.; Mehrali, M.; Metselaar, H.S.C.; Silakhori, M. Shape-stabilized phase change materials with high thermal conductivity based on paraffin/graphene oxide composite. *Energy Convers. Manag.* **2013**, *67*, 275–282. [CrossRef]

45. Chung, D.D.L. Thermal interface materials. *J. Mater. Eng. Perform.* **2001**, *10*, 56–59. [CrossRef]

46. Karaıpeklı, A.; Sarı, A.; Kaygusuz, K. Thermal characteristics of paraffin/expanded perlite composite for latent heat thermal energy storage. *Energy Sources A* **2009**, *31*, 814–823. [CrossRef]

47. Garg, H.P.; Mullick, S.C.; Bhargava, A.K. Latent Heat or Phase Change Thermal Energy Storage. In *Solar Thermal Energy Storage*; Springer: Berlin, Germany, 1985; pp. 154–291.

48. Hasan, A.; McCormack, S.J.; Huang, M.J.; Norton, B. Evaluation of phase change materials for thermal regulation enhancement of building integrated photovoltaics. *Sol. Energy* **2010**, *84*, 1601–1612. [CrossRef]

49. Stekli, J.; Irwin, L.; Pitchumani, R. Technical challenges and opportunities for concentrating solar power with thermal energy storage. *J. Therm. Sci. Eng. Appl.* **2013**, *5*, 021011. [CrossRef]

50. Ungar, G.; Keller, A. Long range intermixing of paraffin molecules in the crystalline state. *Colloid Polym. Sci.* **1979**, *257*, 90–94. [CrossRef]

51. Navarro, L.; de Gracia, A.; Castell, A.; Cabeza, L.F. Thermal behaviour of insulation and phase change materials in buildings with internal heat loads: Experimental study. *Energy Effic.* **2015**, *8*, 895–904. [CrossRef]

52. Li, M. A nano-graphite/paraffin phase change material with high thermal conductivity. *Appl. Energy* **2013**, *106*, 25–30. [CrossRef]

53. Ettouney, H.; El-Dessouky, H.; Al-Ali, A. Heat transfer during phase change of paraffin wax stored in spherical shells. *J. Sol. Energy Eng.* **2005**, *127*, 357–365. [CrossRef]

54. Zhang, X.; Tian, J.; Wang, L.; Zhou, Z. Wettability effect of coatings on drag reduction and paraffin deposition prevention in oil. *J. Pet. Sci. Eng.* **2002**, *36*, 87–95. [CrossRef]

55. Sigma-Aldrich, a Part of Merck. Available online: https://www.sigmaaldrich.com/canada-english.html (accessed on 20 August 2016).

56. Albury, A. *Flash Point: A Comparison of PureTemp and Paraffin PCMs*; Entropy Solutions International: Plymouth, MN, USA, 2014.

57. Rao, Z.H.; Wang, S.H.; Zhang, Y.L.; Zhang, G.Q.; Zhang, J.Y. Thermal Properties of Paraffin/Nano-AlN Phase Change Energy Storage Materials. *Energy Sources A Recov. Util. Environ. Eff.* **2014**, *36*, 2281–2286. [CrossRef]

58. Yu, S.; Wang, X.; Wu, D. Microencapsulation of *N*-octadecane phase change material with calcium carbonate shell for enhancement of thermal conductivity and serving durability: Synthesis, microstructure, and performance evaluation. *Appl. Energy* **2014**, *114*, 632–643. [CrossRef]

59. Jin, Z.; Wang, Y.; Liu, J.; Yang, Z. Synthesis and properties of paraffin capsules as phase change materials. *Polymer* **2008**, *49*, 2903–2910. [CrossRef]

60. Yin, D.; Ma, L.; Liu, J.; Zhang, Q. Pickering emulsion: A novel template for microencapsulated phase change materials with polymer–silica hybrid shell. *Energy* **2014**, *64*, 575–581. [CrossRef]

61. Yang, Y.; Ye, X.; Luo, J.; Song, G.; Liu, Y.; Tang, G. Polymethyl methacrylate based phase change microencapsulation for solar energy storage with silicon nitride. *Sol. Energy* **2015**, *115*, 289–296. [CrossRef]

62. Kośny, J. *Analysis of the Dynamic Thermal Performance of Fiberous Insulations Containing Phase Change Materials*; Oak Ridge National Laboratory: Oak Ridge, TN, USA, 2009.

63. Cui, Y.; Liu, C.; Hu, S.; Yu, X. The experimental exploration of carbon nanofiber and carbon nanotube additives on thermal behavior of phase change materials. *Sol. Energy Mater. Sol. Cells* **2011**, *95*, 1208–1212. [CrossRef]

64. Serrano, S.; Barreneche, C.; Rincón, L.; Boer, D.; Cabeza, L.F. Optimization of three new compositions of stabilized rammed earth incorporating PCM: Thermal properties characterization and LCA. *Constr. Build. Mater.* **2013**, *47*, 872–878. [CrossRef]

65. Lai, C.M.; Hokoi, S. Thermal performance of an aluminum honeycomb wallboard incorporating microencapsulated PCM. *Energy Build.* **2014**, *73*, 37–47. [CrossRef]

66. Kheradmand, M.; Azenha, M.; de Aguiar, J.L.; Krakowiak, K.J. Thermal behavior of cement based plastering mortar containing hybrid microencapsulated phase change materials. *Energy Build.* **2014**, *84*, 526–536. [CrossRef]

67. Jeong, S.G.; Jeon, J.; Seo, J.; Lee, J.H.; Kim, S. Performance evaluation of the microencapsulated PCM for wood-based flooring application. *Energy Convers. Manag.* **2012**, *64*, 516–521. [CrossRef]

68. Li, Z.; Sun, W.G.; Wang, G.; Wu, Z.G. Experimental and numerical study on the effective thermal conductivity of paraffin/expanded graphite composite. *Sol. Energy Mater. Sol. Cells* **2014**, *128*, 447–455. [CrossRef]

69. Fan, L.W.; Fang, X.; Wang, X.; Zeng, Y.; Xiao, Y.Q.; Yu, Z.T.; Cen, K.F. Effects of various carbon nanofillers on the thermal conductivity and energy storage properties of paraffin-based nanocomposite phase change materials. *Appl. Energy* **2013**, *110*, 163–172. [CrossRef]

70. Chen, F.; Wolcott, M. Polyethylene/paraffin binary composites for phase change material energy storage in building: A morphology, thermal properties, and paraffin leakage study. *Sol. Energy Mater. Sol. Cells* **2015**, *137*, 79–85. [CrossRef]

71. Zhang, H.; Wang, X.; Wu, D. Silica encapsulation of *N*-octadecane via sol–gel process: A novel microencapsulated phase-change material with enhanced thermal conductivity and performance. *J. Colloid Interface Sci.* **2010**, *343*, 246–255. [CrossRef] [PubMed]

72. He, F.; Wang, X.; Wu, D. New approach for sol–gel synthesis of microencapsulated *N*-octadecane phase change material with silica wall using sodium silicate precursor. *Energy* **2014**, *67*, 223–233. [CrossRef]

73. Özonur, Y.; Mazman, M.; Paksoy, H.Ö.; Evliya, H. Microencapsulation of coco fatty acid mixture for thermal energy storage with phase change material. *Int. J. Energy Res.* **2006**, *30*, 741–749. [CrossRef]

74. He, H.; Zhao, P.; Yue, Q.; Gao, B.; Yue, D.; Li, Q. A novel polynary fatty acid/sludge ceramsite composite phase change materials and its applications in building energy conservation. *Renew. Energy* **2015**, *76*, 45–52. [CrossRef]

75. Sharma, A.; Shukla, A.; Chen, C.R.; Dwivedi, S. Development of phase change materials for building applications. *Energy Build.* **2013**, *64*, 403–407. [CrossRef]

76. Tang, F.; Cao, L.; Fang, G. Preparation and thermal properties of stearic acid/titanium dioxide composites as shape-stabilized phase change materials for building thermal energy storage. *Energy Build.* **2014**, *80*, 352–357. [CrossRef]

77. Chen, Z.; Cao, L.; Shan, F.; Fang, G. Preparation and characteristics of microencapsulated stearic acid as composite thermal energy storage material in buildings. *Energy Build.* **2013**, *62*, 469–474. [CrossRef]

78. Konuklu, Y.; Unal, M.; Paksoy, H.O. Microencapsulation of caprylic acid with different wall materials as phase change material for thermal energy storage. *Sol. Energy Mater. Sol. Cells* **2014**, *120*, 536–542. [CrossRef]

79. Garg, H.P.; Mullick, S.C.; Bhargava, V.K. *Solar Thermal Energy Storage*; Springer Science & Business Media: Berlin, Germany, 2012.

80. U.S. Environmental Protection Agency (EPA). 2016. Available online: http://actor.epa.gov/actor/faces/Assay.jsp (accessed on 5 January 2016).

81. Government of Dubai. *Green Building Regulations & Specifications*; Government of Dubai: Dubai, UAE, 2011.

82. Sarı, A.; Kaygusuz, K. Some fatty acids used for latent heat storage: Thermal stability and corrosion of metals with respect to thermal cycling. *Renew. Energy* **2003**, *28*, 939–948. [CrossRef]

83. Lin, W.; Ma, Z.; Sohel, M.I.; Cooper, P. Development and evaluation of a ceiling ventilation system enhanced by solar photovoltaic thermal collectors and phase change materials. *Energy Convers. Manag.* **2014**, *88*, 218–230. [CrossRef]

84. PAN Pesticides Database—Chemicals. Available online: http://www.pesticideinfo.org/Detail_Chemical.jsp?Rec_Id=PC33152#Toxicity (accessed on 5 January 2016).

85. Ku, W.H.; Lau, D.C.Y.; Huen, K.F. Probiotics Provoked D-lactic Acidosis in Short Bowel Syndrome: Case Report and Literature Review. *HK J. Paediatr.* **2006**, *11*, 246–254.

86. Patil, G. Review of phase change materials useful for thermal storage system. *Glob. J. Adv. Eng. Technol. Sci.* **2015**, *11*, 1–5.

87. Townsend Letter. 2015. Available online: http://www.townsendletter.com/Jan2015/green0115.html (accessed on 5 January 2016).

88. NingxiaJiafeng Chemicals Co., Ltd. Available online: http://jiafengchem.com.cn/en/product_detail.aspx?ProductsCateID=60&ProductsID=21&gclid=CPKgtf69ksoCFSfkwgoda0YLug (accessed on 5 January 2016).

89. CAMEO Chemicals. Available online: http://cameochemicals.noaa.gov/chemical/22150 (accessed on 5 January 2016).

90. Bhatt, V.D.; Gohil, K.; Mishra, A. Thermal energy storage capacity of some phase changing materials and ionic liquids. *Int. J. ChemTech Res.* **2010**, *2*, 1771e9.

91. Norton, B. *Harnessing Solar Heat*; Springer: Berlin, Germany, 2014.

92. Veerappan, M.; Kalaiselvam, S.; Iniyan, S.; Goic, R. Phase change characteristic study of spherical PCMs in solar energy storage. *Sol. Energy* **2009**, *83*, 1245–1252. [CrossRef]

93. PCM Price Challenge. Available online: https://cdn2.hubspot.net/hub/55819/file-30934935-pdf/docs/pcm_price_challenge.pdf (accessed on 20 June 2016).

94. Gawron, K.; Schröder, J. Properties of some salt hydrates for latent heat storage. *Int. J. Energy Res.* **1977**, *1*, 351–363. [CrossRef]

95. Berroug, F.; Lakhal, E.K.; El Omari, M.; Faraji, M.; El Qarnia, H. Thermal performance of a greenhouse with a phase change material north wall. *Energy Build.* **2011**, *43*, 3027–3035. [CrossRef]

96. Zhou, D.; Zhao, C.Y. Experimental investigations on heat transfer in phase change materials (PCMs) embedded in porous materials. *Appl. Therm. Eng.* **2011**, *31*, 970–977. [CrossRef]

97. N'Tsoukpoe, K.; Rammelberg, H.U.; Lele, A.F.; Korhammer, K.; Watts, B.A.; Schmidt, T.; Wolfgang, K.L. A review on the use of calcium chloride in applied thermal engineering. *Appl. Therm. Eng.* **2015**, *75*, 513–531. [CrossRef]

98. Sharma, S.D.; Kitano, H.; Sagara, K. Phase change materials for low temperature solar thermal applications. *Res. Rep. Fac. Eng.* **2004**, *29*, 31–64.

99. Gruszkiewicz, M.S.; Simonson, J.M. Vapor pressures and isopiestic molalities of concentrated $CaCl_2(aq)$, $CaBr_2(aq)$, and $NaCl(aq)$. *J. Chem. Thermodyn.* **2005**, *37*, 906–930. [CrossRef]

100. Kenisarin, M.; Mahkamov, K. Salt hydrates as latent heat storage materials: Thermophysical properties and costs. *Sol. Energy. Mater. Sol. Cells* **2016**, *145*, 255–286. [CrossRef]

101. Tyagi, V.V.; Buddhi, D. Thermal cycle testing of calcium chloride hexahydrate as a possible PCM for latent heat storage. *Sol. Energy. Mater. Sol. Cells* **2008**, *92*, 891–899. [CrossRef]

102. Kaygusuz, K. Experimental and theoretical investigation of latent heat storage for water based solar heating systems. *Energy Convers. Manag.* **1995**, *36*, 315–323. [CrossRef]

103. Cabeza, L.F.; Illa, J.; Roca, J.; Badia, F.; Mehling, H.; Hiebler, S. Middle term immersion corrosion tests on metal-salt hydrate pairs used for latent heat storage in the 32 to 36 °C temperature range. *Mater. Corros.* **2001**, *52*, 748–754. [CrossRef]

104. Lane, G.A. *Macro-Encapsulation of PCM*; Report No. ORO/5117-8; Dow Chemical Company: Midland, MI, USA, 1978.

105. Biswas, R. Thermal storage using sodium sulfate decahydrate and water. *Sol. Energy* **1977**, *99*, 99–100. [CrossRef]

106. Charlsson, B.; Stymme, H.; Wattermark, G. An incongruent heat of fusion system $CaCl_26H_2O$ made congruent through modification of chemical composition of the system. *Sol. Energy* **1979**, *23*, 343–350.

107. Alexiades, V.; Solomon Alan, D. *Mathematical Modeling of Melting and Freezing Process*; Hemisphere Publishing Corporation: Washington, DC, USA, 1992.

108. Lane, G.A.; Rossow, H.E. Encapsulation of heat of fusion storage materials. In Proceedings of the Second South Eastern Conference on Application of Solar Energy, Baton Rouge, LA, USA, 19–22 April 1976; pp. 442–455.

109. Telkes, M. Thermal storage for solar heating and cooling. In Proceedings of the Workshop on Solar Energy Storage Sub-Systems for Heating and Cooling of Buildings, Charlottesville, VA, USA, 16–18 April 1975.

110. Telkes, M. Nucleation of super saturated inorganic salt solution. *Ind. Eng. Chem.* **1952**, *44*, 1308–1310. [CrossRef]

111. Leoni, N.; Amon, C.H. Transient thermal design of wearable computers with embedded electronics using phase change materials. In Proceedings of the 32nd ASME National Heat Transfer Conference, Baltimore, MD, USA, 8–12 August 1997; pp. 49–56.

112. Hadjieva, M.; Stoykov, R.; Filipova, T.Z. Composite salt-hydrate concrete system for building energy storage. *Renew. Energy* **2000**, *19*, 111–115. [CrossRef]

113. Lee, K.O.; Medina, M.A.; Raith, E.; Sun, X. Assessing the integration of a thin phase change material (PCM) layer in a residential building wall for heat transfer reduction and management. *Appl. Energy* **2015**, *137*, 699–706. [CrossRef]

114. Zhong, L.; Zhang, X.; Luan, Y.; Wang, G.; Feng, Y.; Feng, D. Preparation and thermal properties of porous heterogeneous composite phase change materials based on molten salts/expanded graphite. *Sol. Energy* **2014**, *107*, 63–73. [CrossRef]

115. Huang, J.; Wang, T.; Zhu, P.; Xiao, J. Preparation, characterization, and thermal properties of the microencapsulation of a hydrated salt as phase change energy storage materials. *Thermochim. Acta* **2013**, *557*, 1–6. [CrossRef]

116. Su, W.; Darkwa, J.; Kokogiannakis, G. Review of solid–liquid phase change materials and their encapsulation technologies. *Renew. Sustain. Energy Rev.* **2015**, *48*, 373–391. [CrossRef]
117. Kumar, R.; Misra, M.K.; Kumar, R.; Gupta, D.; Khatri, P.K.; Tak, B.B.; Meena, S.R. Phase Change Materials: Technology Status and Potential Defence Applications (Review Papers). *Def. Sci. J.* **2011**, *61*, 576–582. [CrossRef]
118. Ma, K.; Liu, J. Liquid metal cooling in thermal management of computer chips. *Front. Energy Power Eng. China* **2007**, *1*, 384–402. [CrossRef]
119. Deng, Y.; Liu, J. A liquid metal cooling system for the thermal management of high power LEDs. *Int. Commun. Heat Mass Transf.* **2010**, *37*, 788–791. [CrossRef]
120. Li, H.; Liu, J. Revolutionizing heat transport enhancement with liquid metals: Proposal of a new industry of water-free heat exchangers. *Front. Energy* **2011**, *5*, 20–42. [CrossRef]
121. Li, P.; Liu, J. Harvesting low grade heat to generate electricity with thermosyphon effect of room temperature liquid metal. *Appl. Phys. Lett.* **2011**, *99*, 094106. [CrossRef]
122. Dai, D.; Zhou, Y.; Liu, J. Liquid metal based thermoelectric generation system for waste heat recovery. *Renew. Energy* **2011**, *36*, 3530–3536. [CrossRef]
123. Zhang, Q.; Liu, J. Nano liquid metal as an emerging functional material in energy management, conversion and storage. *Nano Energy* **2013**, *2*, 863–872. [CrossRef]
124. BASF SE. Available online: http://www.micronal.de/portal/load/fid774774/Catalogue%20Micronal%20PCM.pdf (accessed on 9 March 2016).
125. Rubitherm Technologies GmbH. Available online: http://www.rubitherm.eu/produktkategorien.html (accessed on 9 March 2016).
126. Microtek Laboratories, Inc. Available online: http://www.microteklabs.com/data-sheets.html (accessed on 9 March 2016).
127. SavEnrg™ Phase Change Material. Available online: http://rgees.com/products.php (accessed on 9 March 2016).
128. Phase Change Products Pty Ltd. (PCP). Available online: http://pcpaustralia.com.au/ (accessed on 9 March 2016).
129. PCM Energy P. Ltd. Available online: http://pcmenergy.com/products.htm (accessed on 9 March 2016).
130. Phase Change Material Products Limited. Available online: http://www.pcmproducts.net/Phase_Change_Material_Products.htm (accessed on 9 March 2016).
131. Climator Sweden AB. Available online: http://climator.com/room-en/?lang=en (accessed on 9 March 2016).
132. Salca BV. Available online: http://www.salcabv.nl/index.asp?CategorieID=2&Taal=EN (accessed on 9 March 2016).
133. Entropy Solutions, LLC. Available online: http://www.puretemp.com/stories/puretemp-technical-data-sheets (accessed on 9 March 2016).
134. Karthikeyan, M.; Ramachandran, T. Review of thermal energy storage of micro-and nanoencapsulated phase change materials. *Mater. Res. Innov.* **2014**, *18*, 541–554. [CrossRef]
135. Ukrainczyk, N.; Kurajica, S.; Šipušić, J. Thermophysical comparison of five commercial paraffin waxes as latent heat storage materials. *Chem. Biochem. Eng. Q.* **2010**, *24*, 129–137.
136. Kalinov, B.P.; Pereverzev, A.N.; Pivovarov, A.T.; Shtapova, V.K. Interconnection of the parameters of the quality of a paraffin distillate from ozerksuatsk petroleum. *Chem. Technol. Fuels Oils* **1968**, *4*, 331–334. [CrossRef]
137. Yuan, Y.; Lee, T.R. Contact angle and wetting properties. In *Surface Science Techniques*; Springer: Berlin/Heidelberg, Germany, 2013; pp. 3–34.
138. Sohns, J.; Seifert, B.; Hahne, E. The effect of impurities on the melting temperature and the heat of fusion of latent heat storage materials. *Int. J. Thermophys.* **1981**, *2*, 71–87. [CrossRef]
139. Cabeza, L.F.; Mehling, H. Solid-Liquid Phase Change Materials. In *Heat and Cold Storage with PCM—An Up to Date Introduction into Basics and Applications*; Springer: Berlin, Germany, 2008; p. 308.
140. Sandnes, B.; Rekstad, J. Supercooling salt hydrates: Stored enthalpy as a function of temperature. *Sol. Energy* **2006**, *80*, 616–625. [CrossRef]
141. Galwey, A.K.; Brown, M.E. *Thermal Decomposition of Ionic Solids: Chemical Properties and Reactivities of Ionic Crystalline Phases*; Elsevier: Amsterdam, The Netherlands, 1999; Volume 86.

142. Kenisarin, M.; Mahkamov, K. Solar energy storage using phase change materials. *Renew. Sustain. Energy Rev.* **2007**, *11*, 1913–1965. [CrossRef]

143. Umer, H.; Nigam, H.; Tamboli, A.M.; Nainar, M.S.M. Microencapsulation: Process, techniques and applications. *Int. J. Res. Pharm. Biomed. Sci.* **2011**, *2*, 474–480.

144. Xing, J.; Li, Y.; Newton, E.; Yeung, K.-W. Method for Encapsulating Paraffin Compounds that Can Undergo Phase Transitional and Microcapsule Resulting Therefrom. Patent WO 2003099427 A1, 4 December 2003.

145. Liang, C.; Lingling, X.; Hongbo, S.; Zhibin, Z. Microencapsulation of butyl stearate as a phase change material by interfacial polycondensation in a polyurea system. *Energy Convers. Manag.* **2009**, *50*, 723–729. [CrossRef]

146. Cho, J.S.; Kwon, A.; Cho, C.G. Microencapsulation of octadecane as a phase-change material by interfacial polymerization in an emulsion system. *Colloid Polym. Sci.* **2002**, *280*, 260–266. [CrossRef]

147. Saihi, D.; Vroman, I.; Giraud, S.; Bourbigot, S. Microencapsulation of ammonium phosphate with a polyurethane shell. Part II. Interfacial polymerization technique. *React. Funct. Polym.* **2006**, *66*, 1118–1125. [CrossRef]

148. Salaün, F.; Bedek, G.; Devaux, E.; Dupont, D.; Gengembre, L. Microencapsulation of a cooling agent by interfacial polymerization: Influence of the parameters of encapsulation on poly (urethane–urea) microparticles characteristics. *J. Membr. Sci.* **2011**, *370*, 23–33. [CrossRef]

149. Lu, S.; Xing, J.; Zhang, Z.; Jia, G. Preparation and characterization of polyurea/polyurethane double-shell microcapsules containing butyl stearate through interfacial polymerization. *J. Appl. Polym. Sci.* **2011**, *121*, 3377–3383. [CrossRef]

150. Su, J.F.; Wang, L.X.; Ren, L.; Huang, Z.; Meng, X.W. Preparation and characterization of polyurethane microcapsules containing *n*-octadecane with styrene-maleic anhydride as a surfactant by interfacial polycondensation. *J. Appl. Polym. Sci.* **2006**, *102*, 4996–5006. [CrossRef]

151. Siddhan, P.; Jassal, M.; Agrawal, A.K. Core content and stability of *n*-octadecane-containing polyurea microencapsules produced by interfacial polymerization. *J. Appl. Polym. Sci.* **2007**, *106*, 786–792. [CrossRef]

152. Microencapsulation. Available online: https://uqu.edu.sa/files2/tiny_mce/plugins/filemanager/files/4290121/MICROENCAPSULATION.pdf (accessed on 29 February 2016).

153. Swapan, K.G. *Functional Coatings by Polymer Microencapsulation*; Wiley-VCH: Weinheim, Germany, 2006.

154. You, M.; Zhang, X.X.; Li, W.; Wang, X.C. Effects of MicroPCMs on the fabrication of MicroPCMs/polyurethane composite foams. *Thermochim. Acta* **2008**, *472*, 20–24. [CrossRef]

155. Sarier, N.; Onder, E. The manufacture of microencapsulated phase change materials suitable for the design of thermally enhanced fabrics. *Thermochim Acta* **2007**, *452*, 149–160. [CrossRef]

156. Lee, S.H.; Yoon, S.J.; Kim, Y.G.; Choi, Y.C.; Kim, J.H.; Lee, J.G. Development of building materials by using micro-encapsulated phase change material. *Korean J. Chem. Eng.* **2007**, *24*, 332–335. [CrossRef]

157. Boh, B.; Knez, E.; Staresinic, M. Microencapsulation of higher hydrocarbon phase change materials by in situ polymerization. *J. Microencapsul.* **2005**, *22*, 715–735. [CrossRef] [PubMed]

158. Fang, G.; Li, H.; Yang, F.; Liu, X.; Wu, S. Preparation and characterization of nano-encapsulated *N*-tetradecane as phase change material for thermal energy storage. *Chem. Eng. J.* **2009**, *153*, 217–221. [CrossRef]

159. Hu, X.; Huang, Z.; Yu, X.; Li, B. Preparation and thermal energy storage of carboxymethyl cellulose-modified nanocapsules. *BioEnergy Res.* **2013**, *6*, 1135–1141. [CrossRef]

160. Karthikeyan, M.; Ramachandran, T.; Sundaram, O.S. Nanoencapsulated phase change materials based on polyethylene glycol for creating thermoregulating cotton. *J. Ind. Text.* **2014**, *44*, 130–146. [CrossRef]

161. Fei, X.; Zhao, H.; Zhang, B.; Cao, L.; Yu, M.; Zhou, J.; Yu, L. Microencapsulation mechanism and size control of fragrance microcapsules with melamine resin shell. *Colloids Surf. A Physicochem. Eng. Asp.* **2015**, *469*, 300–306. [CrossRef]

162. Benita, S. *Microencapsulation: Methods and Industrial Applications*; CRC Press: Boca Raton, FL, USA, 2005.

163. Saihi, D.; Vroman, I.; Giraud, S.; Bourbigot, S. Microencapsulation of ammonium phosphate with a polyurethane shell part I: Coacervation technique. *React. Funct. Polym.* **2005**, *64*, 127–138. [CrossRef]

164. Jamekhorshid, A.; Sadrameli, S.M.; Farid, M. A review of microencapsulation methods of phase change materials (PCMs) as a thermal energy storage (TES) medium. *Renew. Sustain. Energy Rev.* **2014**, *31*, 531–542. [CrossRef]

165. Mishra, M. *Handbook of Encapsulation and Controlled Release*; CRC Press: Boca Raton, FL, USA, 2015.

166. Piacentini, E.; Giorno, L.; Dragosavac, M.M.; Vladisavljević, G.T.; Holdich, R.G. Microencapsulation of oil droplets using cold water fish gelatine/gum arabic complex coacervation by membrane emulsification. *Food Res. Int.* **2013**, *53*, 362–372. [CrossRef]

167. Onder, E.; Sarier, N.; Cimen, E. Encapsulation of phase change materials by complex coacervation to improve thermal performances of woven fabrics. *Thermochim. Acta* **2008**, *467*, 63–72. [CrossRef]

168. Mayya, K.S.; Bhattacharyya, A.; Argillier, J.F. Micro-encapsulation by complex coacervation: Influence of surfactant. *Polym. Int.* **2003**, *52*, 644–647. [CrossRef]

169. Su, J.F.; Huang, Z.; Ren, L. High compact melamine-formaldehyde microPCMs containing *N*-octadecane fabricated by a two-step coacervation method. *Colloid Polym. Sci.* **2007**, *285*, 1581–1591. [CrossRef]

170. Cao, L.; Tang, F.; Fang, G. Synthesis and characterization of microencapsulated paraffin with titanium dioxide shell as shape-stabilized thermal energy storage materials in buildings. *Energy Build.* **2014**, *72*, 31–37. [CrossRef]

171. Pan, W.; Ye, J.; Ning, G.; Lin, Y.; Wang, J. A novel synthesis of micrometer silica hollow sphere. *Mater. Res. Bull.* **2009**, *44*, 280–283. [CrossRef]

172. Zhang, H.; Wu, J.; Zhou, L.; Zhang, D.; Qi, L. Facile synthesis of monodisperse microspheres and gigantic hollow shells of mesoporous silica in mixed water-ethanol solvents. *Langmuir* **2007**, *23*, 1107–1113. [CrossRef] [PubMed]

173. Deng, Z.; Chen, M.; Zhou, S.; You, B.; Wu, L. A novel method for the fabrication of monodisperse hollow silica spheres. *Langmuir* **2006**, *22*, 6403–6407. [CrossRef] [PubMed]

174. Cape, S.P.; Villa, J.A.; Huang, E.T.; Yang, T.H.; Carpenter, J.F.; Sievers, R.E. Preparation of active proteins, vaccines and pharmaceuticals as fine powders using supercritical or near-critical fluids. *Pharm. Res.* **2008**, *25*, 1967–1990. [CrossRef] [PubMed]

175. Campardelli, R.; Oleandro, E.; Reverchon, E. Supercritical assisted injection in a liquid antisolvent for PLGA and PLA microparticle production. *Powder Technol.* **2016**, *287*, 12–19. [CrossRef]

176. Campardelli, R.; Santo, I.E.; Albuquerque, E.C.; de Melo, S.V.; Della Porta, G.; Reverchon, E. Efficient encapsulation of proteins in submicro liposomes using a supercritical fluid assisted continuous process. *J. Supercrit. Fluids* **2016**, *107*, 163–169. [CrossRef]

177. Ivanovic, J.; Milovanovic, S.; Zizovic, I. Utilization of supercritical CO_2 as a processing aid in setting functionality of starch-based materials. *Starch-Stärke* **2016**, *68*, 821–833. [CrossRef]

178. Jyothi, S.S.; Seethadevi, A.; Prabha, K.S.; Muthuprasanna, P.; Pavitra, P. Microencapsulation: A review. *Int. J. Pharm. Biol. Sci.* **2012**, *3*, 509–531.

179. Fages, J.; Lochard, H.; Letourneau, J.J.; Sauceau, M.; Rodier, E. Particle generation for pharmaceutical applications using supercritical fluid technology. *Powder Technol.* **2004**, *141*, 219–226. [CrossRef]

180. Venkatesan, P.; Manavalan, R.; Valliappan, K. Microencapsulation: A vital technique in novel drug delivery system. *J. Pharm. Sci. Res.* **2009**, *1*, 26–35.

181. O'Donnell, P.B.; McGinity, J.W. Preparation of microspheres by the solvent evaporation technique. *Adv. Drug Deliv. Rev.* **1997**, *28*, 25–42. [CrossRef]

182. Yang, Y.Y.; Chia, H.H.; Chung, T.S. Effect of preparation temperature on the characteristics and release profiles of PLGA microspheres containing protein fabricated by double-emulsion solvent extraction/evaporation method. *J. Control. Release* **2000**, *69*, 81–96. [CrossRef]

183. Khamanga, S.M.; Parfitt, N.; Nyamuzhiwa, T.; Haidula, H.; Walker, R.B. The evaluation of eudragit microcapsules manufactured by solvent evaporation using USP apparatus 1. *Dissolut. Technol.* **2009**, *16*, 15–22. [CrossRef]

184. Gravalos, G.M.; Ignacio, C.H.; Juan, M.R.; Jose, C.C.; Ana María, B.S.; Manuel, C.F.; Juan, F.; José, L. Procedure for Microencapsulation of Phase Change Materials by Spray-Drying. Europe Patent EP 2119498 A1, 18 November 2009.

185. Borreguero, A.M.; Valverde, J.L.; Rodríguez, J.F.; Barber, A.H.; Cubillo, J.J.; Carmona, M. Synthesis and characterization of microcapsules containing Rubitherm® RT27 obtained by spray drying. *Chem. Eng. J.* **2011**, *166*, 384–390. [CrossRef]

186. Okuyama, K.; Abdullah, M.; Lenggoro, I.W.; Iskandar, F. Preparation of functional nanostructured particles by spray drying. *Adv. Powder Technol.* **2006**, *17*, 587–611. [CrossRef]

187. Chávarri, M.; Marañón, I.; Villarán, M.C. *Encapsulation Technology to Protect Probiotic Bacteria*; INTECH Open Access Publisher: Miñano, Spain, 2012.

188. Ushak, S.; Cruz, M.J.; Cabeza, L.F.; Grágeda, M. Preparation and Characterization of Inorganic PCM Microcapsules by Fluidized Bed Method. *Materials* **2016**, *9*, 24. [CrossRef]

189. Desai, K.G.H.; Jin Park, H. Recent developments in microencapsulation of food ingredients. *Dry. Technol.* **2005**, *23*, 1361–1394. [CrossRef]

190. Feng, T.; Xiao, Z.; Tian, H. Recent patents in flavor microencapsulation. *Recent Pat. Food Nutr. Agric.* **2009**, *1*, 193–202. [CrossRef] [PubMed]

191. Gouin, S. Microencapsulation: Industrial appraisal of existing technologies and trends. *Trends Food Sci. Technol.* **2004**, *15*, 330–347. [CrossRef]

192. Werner, S.R.; Jones, J.R.; Paterson, A.H.; Archer, R.H.; Pearce, D.L. Air-suspension particle coating in the food industry: Part I—State of the art. *Powder Technol.* **2007**, *171*, 25–33. [CrossRef]

193. Werner, S.R.; Jones, J.R.; Paterson, A.H.; Archer, R.H.; Pearce, D.L. Air-suspension coating in the food industry: Part II—Micro-level process approach. *Powder Technol.* **2007**, *171*, 34–45. [CrossRef]

194. Vandegaer, J.E. *Microencapsulation: Processes and Applications*; Springer Science & Business Media: Berlin, Germany, 2012.

195. Tarun, G.; Murthy, R.S.R. Patented microencapsulation techniques and its application. *J. Pharm. Res.* **2011**, *4*, 2097–2102.

196. Versic, R.J. Pharmaceuticals Microencapsulated by Vapor Deposited Polymers and Method. U.S. Patent 5288504 A, 22 February 1994.

197. Palmer, S.; Seville, J.; Ingram, A.; Fitzpatrick, S.; Fan, X. Tracking pellet motion in a Wurster coater using positron emission. In Proceedings of the 2006 AIChE Spring National Meeting—5th World Congress on Particle Technology (Session# 158b), Orlando, FL, USA, 23–27 April 2006.

198. Fichana, D.; Marchut, A.J.; Ohlsson, P.H.; Chang, S.Y.; Lyngberg, O.; Dougherty, J.; Muzzio, F. Experimental and model-based approaches to studying mixing in coating pans. *Pharm. Dev. Technol.* **2009**, *14*, 173–184. [CrossRef] [PubMed]

199. Cunningham, C.; Hansell, J.; Nuneviller, F., III; Rajabi-Siahboomi, A.R. Evaluation of recent advances in continuous film coating processes. *Drug Dev. Ind. Pharm.* **2010**, *36*, 227–233. [CrossRef] [PubMed]

200. Clark, J.P. *Practical Design, Construction and Operation of Food Facilities*; Academic Press: Cambridge, MA, USA, 2008.

201. Salaün, F.; Devaux, E.; Bourbigot, S.; Rumeau, P. Influence of process parameters on microcapsules loaded with *N*-hexadecane prepared by in situ polymerization. *Chem. Eng. J.* **2009**, *155*, 457–465. [CrossRef]

202. Latibari, S.T.; Mehrali, M.; Mehrali, M.; Mahlia, T.M.I.; Metselaar, H.S.C. Synthesis, characterization and thermal properties of nanoencapsulated phase change materials via sol–gel method. *Energy* **2013**, *61*, 664–672. [CrossRef]

203. Thiele, A.M.; Kumar, A.; Sant, G.; Pilon, L. Effective thermal conductivity of three-component composites containing spherical capsules. *Int. J. Heat Mass Transf.* **2014**, *73*, 177–185. [CrossRef]

204. Darkwa, K. Quasi-isotropic laminated phase-change material system. *Appl. Energy* **2007**, *84*, 599–607. [CrossRef]

205. Zhou, G.; Yang, Y.; Wang, X.; Cheng, J. Thermal characteristics of shape-stabilized phase change material wallboard with periodical outside temperature waves. *Appl. Energy* **2010**, *87*, 2666–2672. [CrossRef]

206. Pasupathy, A.; Athanasius, L.; Velraj, R.; Seeniraj, R.V. Experimental investigation and numerical simulation analysis on the thermal performance of a building roof incorporating phase change material (PCM) for thermal management. *Appl. Therm. Eng.* **2008**, *28*, 556–565. [CrossRef]

207. Kuznik, F.; Virgone, J.; Roux, J.J. Energetic efficiency of room wall containing PCM wallboard: A full-scale experimental investigation. *Energy Build.* **2008**, *40*, 148–156. [CrossRef]

208. Carbonari, A.; De Grassi, M.; Di Perna, C.; Principi, P. Numerical and experimental analyses of PCM containing sandwich panels for prefabricated walls. *Energy Build.* **2006**, *38*, 472–483. [CrossRef]

209. Alawadhi, E.M. Thermal analysis of a building brick containing phase change material. *Energy Build.* **2008**, *40*, 351–357. [CrossRef]

210. Alawadhi, E.M. Phase change process with free convection in a circular enclosure: Numerical simulations. *Comput. Fluids* **2004**, *33*, 1335–1348. [CrossRef]

211. Darkwa, K.; Kim, J.S. Thermal analysis of composite phase change drywall systems. *J. Sol. Energy Eng.* **2005**, *127*, 352–356. [CrossRef]

212. Li, J.; Xue, P.; He, H.; Ding, W.; Han, J. Preparation and application effects of a novel form-stable phase change material as the thermal storage layer of an electric floor heating system. *Energy Build.* **2009**, *41*, 871–880. [CrossRef]

213. Hunger, M.; Entrop, A.G.; Mandilaras, I.; Brouwers, H.J.H.; Founti, M. The behavior of self-compacting concrete containing micro-encapsulated phase change materials. *Cem. Concr. Compos.* **2009**, *31*, 731–743. [CrossRef]

214. Darkwa, K.; O'Callaghan, P.W. Simulation of phase change drywalls in a passive solar building. *Appl. Therm. Eng.* **2006**, *26*, 853–858. [CrossRef]

215. Heim, D. Isothermal storage of solar energy in building construction. *Renew. Energy* **2010**, *35*, 788–796. [CrossRef]

216. Kuznik, F.; Virgone, J.; Johannes, K. Development and validation of a new TRNSYS type for the simulation of external building walls containing PCM. *Energy Build.* **2010**, *42*, 1004–1009. [CrossRef]

217. Chandra, S.; Kumar, R.; Kaushik, S.; Kaul, S. Thermal performance of a non-air-conditioned building with PCCM thermal storage wall. *Energy Convers. Manag.* **1985**, *25*, 15–20. [CrossRef]

218. Zhou, G.; Zhang, Y.; Wang, X.; Lin, K.; Xiao, W. An assessment of mixed type PCM-gypsum and shape-stabilized PCM plates in a building for passive solar heating. *Sol. Energy* **2007**, *81*, 1351–1360. [CrossRef]

219. Drissi, S.; Eddhahak, A.; Caré, S.; Neji, J. Thermal analysis by DSC of Phase Change Materials, study of the damage effect. *J. Build. Eng.* **2015**, *1*, 13–19. [CrossRef]

220. Kosny, J.; Kossecka, E.; Brzezinski, A.; Tleoubaev, A.; Yarbrough, D. Dynamic thermal performance analysis of fiber insulations containing bio-based phase change materials (PCMs). *Energy Build.* **2012**, *52*, 122–131. [CrossRef]

221. Kośny, J.; Yarbrough, D.; Wilkes, K.; Leuthold, D.; Syad, A. PCM-Enhanced Cellulose Insulation—Thermal Mass in Lightweight Natural Fibers. In Proceedings of the ECOSTOCK Conference 2006, Pomona, NJ, USA, 31 May–2 June 2006.

222. Pomianowski, M.; Heiselberg, P.; Jensen, R.L. Dynamic heat storage and cooling capacity of a concrete deck with PCM and thermally activated building system. *Energy Build.* **2012**, *53*, 96–107. [CrossRef]

223. Cabeza, L.F.; Navarro Farré, L.; Gracia Cuesta, A.D.; Castell, A.; Álvarez, S. Design of a prefabricated concrete slab with PCM inside the hollows. *Energy Procedia* **2014**, *57*, 2324–2332.